doi:10.1111/ncn3.12033

CASE REPORT

Magnetic resonance imaging findings in Leigh syndrome with a novel compound heterozygous SURF1 gene mutation

Younhee Kim,[1,2] Reiji Koide,[1,2] Eiji Isozaki[1] and Yu-ichi Goto[3]

[1]Department of Neurology, Tokyo Metropolitan Neurological Hospital, Tokyo, [2]Department of Neurology, Jichi Medical University School of Medicine, Shimotsuke, and [3]Department of Mental Retardation and Birth Defect Research, National Institute of Neuroscience, NCNP, Kodaira, Japan

Key words
compound heterozygous mutation, cytochrome c oxydase, Leigh syndrome, leukoencephalopathy, *SURF1*.

Accepted for publication 5 November 2015.

Correspondence
Reiji Koide
Jichi Medical University School of Medicine, 3311-1 Yakushiji, Shimotsuke, Tochigi 329-0498, Japan.
Email: reiji_koide@jichi.ac.jp

Abstract

Leigh syndrome is a severe neurodegenerative disorder that mainly arises in infancy or early childhood. In 1998, mutations in the nuclear *SURF1* gene, which encodes a protein involved in the cytochrome c oxidase, were identified in patients with Leigh syndrome. We report here a patient with Leigh syndrome carrying a novel compound heterozygous mutation in the *SURF1* gene, in whom symmetrical parieto-occipital cortex and white matter lesions were observed by magnetic resonance imaging, in addition to the characteristic basal ganglia lesions in Leigh syndrome.

Introduction

Leigh syndrome (LS) is a severe neurodegenerative disorder, which mainly arises in infancy or early childhood. Its clinical features widely vary, usually consisting of short stature, progressive psychomotor regression and brainstem dysfunction. LS is genetically heterogeneous, and the causative mutations are more than 30. In 1998, mutations in the nuclear *SURF1* gene, which encodes a protein involved in the cytochrome c oxidase (COX), were identified in patients with LS.[1,2] At present, *SURF1* gene mutations are known as the most frequent cause of LS with COX deficiency.[3,4] We report here the case of a patient with LS carrying a compound heterozygous mutation in the *SURF1* gene, in whom symmetrical parieto-occipital cortex and white matter lesions were observed by magnetic resonance imaging, in addition to the characteristic basal ganglia lesions in LS.

Case report

The patient was a 32-year-old man. He was born in breech presentation at 36 weeks of gestation from unrelated parents. The neonatal period was unremarkable. At the age of 1 year and 6 months, he was still not able to walk, and showed failure to thrive and neurodevelopmental retardation. At the age of 2 years, he showed difficulty in maintaining his sitting position. He lost his verbal skills. Laboratory investigations showed an elevated concentration of blood lactate at rest. At the age of 2.5 years, he underwent a muscle biopsy in a local hospital, which showed COX deficiency. He was diagnosed as having LS. At the age of 4 years, he underwent a tracheostomy because of severe pneumonia. Two years later, he required a mechanical ventilator. At this time, he was unable to communicate.

At the age of 27 years, the patient visited to Tokyo Metropolitan Neurological Hospital (Tokyo) to receive home healthcare services. On T2-weighted magnetic resonance images obtained at the age of 29 years, symmetrical hyperintensity lesions in the putamen, olivary nuclei, and parieto-occipital cortex and white matter were observed (Fig. 1a–e). At the age of 32 years, the patient had a disproportionately short stature with short extremities. He presented severe mental retardation and did not respond to attempts at verbal or physical communication. On the basis of the finding of COX deficiency in the previously performed muscle biopsy, we carried out genetic analysis for mitochondrial diseases. Sequence analysis of the *SURF1* gene showed a previously reported substitution mutation (c.737T>A, p.Ile246Asn) in exon 7 in one allele, and a novel frameshift mutation (c.367delA) in exon 5, causing a premature stop codon at amino acid 135 (p.Arg123Glyfs*12) in the other allele. We carried out a polymerase chain reaction assay using allele-specific primers for wild type at c.737 position (c.737T>T) and allele-specific primers for mutant at c.737 position (c.737T>A). Sanger sequencing analysis of polymerase chain reaction products using former primers showed the presence of a c.367delA mutation, whereas, those using

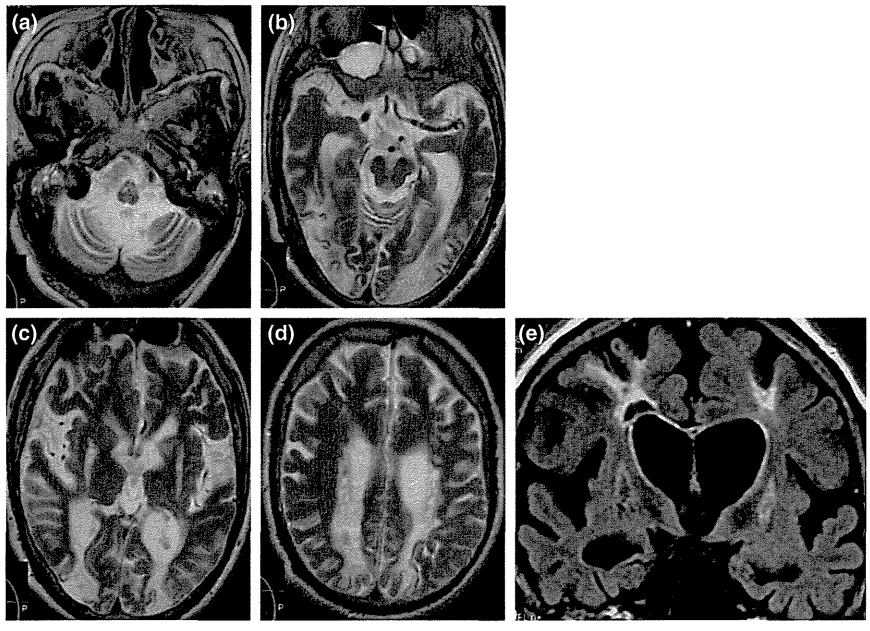

Figure 1 (a–d) T2-weighted images. (e) Fluid-attenuated inversion recovery image. T2-weighted magnetic resonance images show symmetrical high-signal intensity lesions in the (a) olivary nuclei, (c) putamen, and (b–d) cerebral cortex and white matter in the parieto-occipital lobes. (d, e) Some of the white matter lesions appear to be cyst-like.

latter primers found no mutation at the c.367 position. These results suggest that the patient has compound heterozygous mutations.

Discussion

Magnetic resonance imaging patterns in LS with *SURF1* gene mutations have been reported to have the following features: (i) brainstem and subthalamic nuclei lesions might suggest this disorder; (ii) dentate nuclei and substantia nigra are occasionally involved; (iii) basal ganglia lesions are less frequent in LS with *SURF1* mutations than LS without these mutations; and (iv) the absence of putaminal lesions does not exclude the diagnosis of LS.[5,6]

Although leukoencephalopathy has been reported in various forms of mitochondrial diseases, it has rarely been mentioned in LS with *SURF1* mutations.[7,8] Rahman *et al.*[7] reported the case of a LS patient with *SURF1* mutation presenting with symmetrical white matter lesions that appeared as cyst-like lesions in the parieto-occipital lobes. Such characteristics are quite similar to those observed in the present case. The findings in our patient suggest that LS with *SURF1* gene mutations should be considered as one of the differential diagnoses in patients who have lesions in both the basal ganglia and parieto-occipital lobes.

Acknowledgments

The authors declare no conflict of interest.

References

1 Tiranti V, Hoertnagel K, Carronzzo R *et al.* Mutations of SURF-1 in Leigh disease associated with cytochrome c oxidase deficiency. *Am. J. Hum. Genet.* 1998; **63**(6): 1609–21.
2 Zhu Z, Yao J, Johns T *et al.* SURF1, encoding a factor involved in the biogenesis of cytochrome c oxidase, is mutated in Leigh syndrome. *Nat. Genet.* 1998; **20**(4): 337–43.
3 Sue CM, Karadimas C, Checcarelli N *et al.* Differential features of patients with mutations in two COX assembly genes, SURF1 and SCO2. *Ann. Neurol.* 2000; **47**(5): 589–95.
4 Péquignot MO, Dey R, Zeviani M *et al.* Mutation in the SURF1 gene associated with Leigh syndrome and cytochrome C oxidase deficiency. *Hum. Mutat.* 2001; **17**(5): 374–81.
5 Farina L, Chiapparini L, Uziel G *et al.* MR findings in Leigh syndrome with COX deficiency and SURF1 mutations. *Am. J. Neuroradiol.* 2001; **23**(7): 1095–100.
6 Rossi A, Biancheri R, Bruno C *et al.* Leigh syndrome with COX deficiency and SURF1 gene mutations: MR imaging findings. *Am J Neuroradiol* 2003; **24**(6): 1188–91.
7 Rahman S, Brown RM, Chong WK *et al.* A SURF1 gene mutation presenting as isolated leukodystrophy. *Ann. Neurol.* 2001; **49**(6): 797–800.
8 Timothy J, Geller T. SURF-1 gene mutation associated with leukoencephalopathy in a 2-year-old. *J. Child Neurol.* 2009; **24** (10): 1296–301.

Growth Differentiation Factor 15 as a Useful Biomarker for Mitochondrial Disorders

Shuichi Yatsuga, MD, PhD,[1] Yasunori Fujita, PhD,[2] Akiko Ishii, MD, PhD,[3] Yoshihiro Fukumoto, MD, PhD,[4] Hajime Arahata, MD, PhD,[5] Tatsuyuki Kakuma, PhD,[6] Toshio Kojima, MD, PhD,[7] Masafumi Ito, PhD,[2] Masashi Tanaka, MD, PhD,[8] Reo Saiki, MD,[1] and Yasutoshi Koga, MD, PhD[1]

Objective: The diagnosis of mitochondrial disorders (MDs) is occasionally difficult because patients often present with solitary, or a combination of, symptoms caused by each organ insufficiency, which may be the result of respiratory chain enzyme deficiency. Growth differentiation factor 15 (GDF-15) has been reported to be elevated in serum of patients with MDs. In this study, we investigated whether GDF-15 is a more useful biomarker for MDs than several conventional biomarkers.
Methods: We measured the serum levels of GDF-15 and fibroblast growth factor 21 (FGF-21), as well as other biomarkers, in 48 MD patients and in 146 healthy controls in Japan. GDF-15 and FGF-21 concentrations were measured by enzyme-linked immunosorbant assay and compared with lactate, pyruvate, creatine kinase, and the lactate-to-pyruvate ratio. We calculated sensitivity and specificity and also evaluated the correlation based on two rating scales, including the Newcastle Mitochondrial Disease Rating Scale (NMDAS).
Results: Mean GDF-15 concentration was 6-fold higher in MD patients compared to healthy controls (2,711 ± 2,459 pg/ml vs 462.5 ± 141.0 pg/mL; $p < 0.001$). Using a receiver operating characteristic curve, the area under the curve was significantly higher for GDF-15 than FGF-21 and other conventional biomarkers. Our date suggest that GDF-15 is the most useful biomarker for MDs of the biomarkers examined, and it is associated with MD severity.
Interpretation: Our results suggest that measurement of GDF-15 is the most useful first-line test to indicate the patients who have the mitochondrial respiratory chain deficiency.

ANN NEUROL 2015;78:814–823

Mitochondrial disorders (MDs) are occasionally difficult to diagnose because patients present with one or a combination of symptoms, such as psychomotor developmental delay, failure to thrive, short stature, seizures, muscle weakness, hearing loss, heart failure, renal failure, or diabetes. Because the plasma levels of lactate and pyruvate are not always accurate biomarkers or MD diagnosis, a novel biomarker, which is more sensitive, specific, reproducible, and quantitative, is required. Minimizing the number of specimens examined for MD diagnosis is a very important issue for clinicians and/or diagnostic centers in terms of cost- and time-effectiveness.

No reliable biomarker was available for the screening or diagnosis of MDs until 2011.[1] Because an MD

View this article online at wileyonlinelibrary.com. DOI: 10.1002/ana.24506

Received Jan 22, 2015, and in revised form Aug 12, 2015. Accepted for publication Aug 15, 2015.

Address correspondence to Dr Yasutoshi Koga, Department of Pediatrics and Child Health, Kurume University School of Medicine. 67 Asahi-machi, Kurume, Fukuoka 830-0011, Japan.
E-mail: yasukoga@med.kurume-u.ac.jp

From the [1]Department of Pediatrics and Child Health, Kurume University School of Medicine, Fukuoka, Japan; [2]Research Team for Mechanism of Aging, Tokyo Metropolitan Institute of Gerontology, Tokyo, Japan; [3]Department of Neurology, Faculty of Medicine, University of Tsukuba, Ibaraki, Japan; [4]Division of Cardiovascular Medicine, Department of Internal Medicine, Kurume University School of Medicine, Fukuoka, Japan; [5]Department of Neurology, Neuro-Muscular Center, National Omuta Hospital, Fukuoka, Japan; [6]Department of Biostatistics, Kurume University Graduate School of Medicine, Kurume, Japan; [7]Health Care Center, Toyohashi University of Technology, Toyohashi, Japan; and [8]Department of Genomics for Longevity and Health, Tokyo Metropolitan Institute of Gerontology, Tokyo, Japan.

Additional supporting information can be found in the online version of this article.

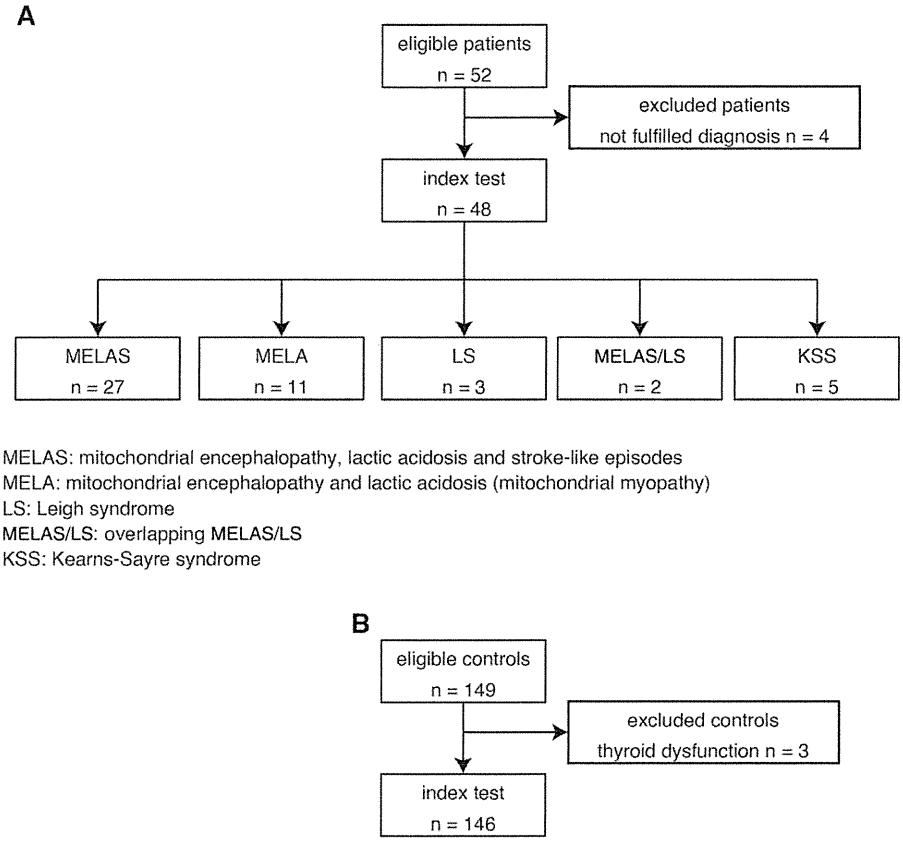

FIGURE 1: STARD flow diagram and demography of the controls, MD patients, and disease controls. (A) All 48 MD patients who fulfilled the clinical diagnostic criteria (mitochondrial encephalopathy, lactic acidosis, and stroke-like episodes [MELAS]; mitochondrial encephalopathy, and lactic acidosis [MELA], for which the main symptom was muscle weakness; Leigh syndrome [LS]; overlapping MELAS/LS; and Kearns-Sayre syndrome [KSS]) and carried a known genetic abnormality were enrolled in this study from 2005 to 2013. (B) Healthy adult and child volunteers without treatment or ambulatory medical care were also recruited in 146 Japanese. MD = mitochondrial disorder; STARD = standards for reporting of diagnostic accuracy.

may present as "any symptom in any organ at any age,"[2] we must develop an optionally useful biomarker for MD diagnosis and the evaluation of therapeutic efficacy. In 2011, serum fibroblast growth factor 21 (FGF-21) was reported to be a useful biomarker for the screening and diagnosis of muscle-manifested MDs.[3,4] The proposed diagnostic process for MDs is as follows: (1) clinical assessment; (2) measurement of the FGF-21 level; (3) long-range polymerase chain reaction, next-generation sequencing, or whole-exome sequencing of nuclear DNA; and (4) with/without histopathological and biochemical analysis via muscle biopsy, which may indicate approximately 70% to 80% of clinically suspected MDs.[5] FGF-21 appears to be a useful novel biomarker for the specific screening of MDs because the measurement of FGF-21 involves a less-invasive approach than muscle biopsy.

Growth differentiation factor 15 (GDF-15) is a member of the transforming growth factor beta superfamily. Expression of GDF-15 in nearly all tissues suggests its general importance in essential cellular functions. GDF-15 has been proposed as a biomarker of heart disease, kidney disease, and cancers; however, its exact biological functions remain poorly understood. It is hypothesized that GDF-15 is elevated by activating transcription factor 4 (ATF4), which is a stress-responsive gene induced by various stresses.[6] GDF-15 is currently under investigation as a marker of the clinical risk factors, mortality, morbidity, and effectiveness of treatments for heart disease, kidney disease, and some cancers; however, GDF-15 does not appear to play a useful role as a diagnostic marker.[7] In 2014, Kalko et al investigated the gene expression profile of TK2-deficient human skeletal muscle using complementary DNA microarrays and demonstrated that serum GDF-15 (GDF-15) may be a novel biomarker for MDs.[8] We performed a microarray analysis of 2SD cybrid cells that harbor a mitochondrial encephalopathy, lactic acidosis, and stroke-like episodes (MELAS)-causing mutation and control cells and demonstrated that expression and secretion of GDF-15 were increased in 2SD cells loaded by lactate; these findings suggest that GDF-15 may serve as a useful marker for MD diagnosis and evaluation of the therapeutic efficacy

TABLE 1. Demographics of the Number, Mean Age, Mean BMI, and % Males for MD Patients and Non-MD Patients

	Controls	MD Patients	Disease Controls
Number	146	48	42
Age, years	23.6 ± 13.7	33.6 ± 18.7**	41.4 ± 17.2***
BMI, kg/m^2 (n)	19.1 ± 3.0 (146)	17.4 ± 3.3 (48)***	21.7 ± 3.8 (41)***
% males (n)	48.0 (70)	48.0 (23)	54.7 (23)

Mean age was significantly higher in MDs patients (33.6 ± 18.7 years old; $p < 0.01$) and disease controls (41.4 ± 17.2 years old; $p < 0.001$) than in healthy controls (23.6 ± 13.7 years old). Mean BMI was significantly lower in MDs patients (17.4 ± 3.3 kg/m^2; $p < 0.001$) than in healthy controls (19.1 ± 3.0 kg/m^2) and higher in disease controls (21.7 ± 3.8 kg/m^2; $p < 0.001$) than in healthy controls (19.1 ± 3.0 kg/m^2). Mann–Whitney *U* test: $^{**}p < 0.01$; $^{***}p < 0.001$.
BMI = body mass index; MD = mitochondrial disorder.

of drugs.[6] In this study, we measured GDF-15 concentrations from patients who suffered from MDs, disease controls, and healthy controls, and evaluated its usefulness for MD diagnosis.

Patients and Methods

Participants

All MD patients who fulfilled the clinical diagnostic criteria (MELAS; mitochondrial encephalopathy, and lactic acidosis [MELA], for which the main symptom was muscle weakness; Leigh syndrome [LS]; overlapping MELAS/LS; and Kearns-Sayre syndrome [KSS]) and carried a known genetic abnormality were enrolled in this study from 2005 to 2013 (Fig 1A). DNA, enzyme, or muscle histopathological analyses were performed on all patients (Supplementary Table 1). The disease controls consisted of adult and child patients with non-MD, including 6 defined Duchenne muscular dystrophy (DMD), 9 multiple sclerosis (MS), 4 anti-AQP4 (aquaporin 4) antibody-positive optic neuritis, 10 limbic encephalitis (anti-GluR [glutamate receptor] antibody-positive, anti-NMDA [N-methyl-D-aspartate] receptor-positive, varicella zoster virus infection, and lung cancer), 1 brainstem encephalitis, 1 meningoencephalitis, 1 SLE (systemic lupus erythematosus) with CNS (central nervous system), 1 NMO (neuromyelitis optica), 1 HUS (hemolytic uremic syndrome) encephalitis, and 8 defined heart failure (HF) patients. All DMD patients were diagnosed with a large deletion of the dystrophin gene by multiplex ligation-dependent probe amplification (MLPA). All MS, optic neuritis, limbic encephalitis, brainstem encephalitis, meningoencephalitis, NMO, and HUS encephalitis patients were diagnosed with fulfilled criteria. All HF patients were diagnosed based on an ejection fraction (EF) below 50% in this study (Supplementary Table 1). Healthy adult and child volunteers without treatment or ambulatory medical care were also recruited from Kurume University Hospital, Fukuoka, Japan (Fig 1B). Mean age, BMI, and % males are shown in Table 1. The study protocol was approved by the institutional review boards of all centers (coordinator: Kurume University Hospital, #13099). Written informed consent was obtained from all subjects before enrollment.

For the healthy controls, we calculated the body mass index (BMI: kg/m^2) of each individual and recruited healthy adults (≥20 years old) who exhibited a BMI between 18 and 25 and children (<20 years old) who exhibited a BMI within ± 2 standard deviations (SDs) of the average for each age in the Japanese population.

Procedures

The serum samples used in this study were collected for analysis from 2012 to 2014. All samples were stored at –80°C until analysis. We measured the GDF-15 (R&D Systems, Minneapolis, USA) and FGF-21 (FGF-21; BioVendor, Brno, Czech Republic) concentrations in duplicate samples by enzyme-linked immunorbent assay (ELISA). The samples for which the concentration of GDF-15 or FGF-21 was higher than the range of detection were diluted 10-fold with dilution buffer and reanalysed. The value from each assay was compared with reference GDF-15 and FGF-21 concentrations. We also measured the levels of conventional biomarkers, such as lactate, pyruvate, the lactate/pyruvate (L/P) ratio, and creatine kinase (CK). In addition, we recorded the height, body weight, BMI, and blood sugar levels. The results of each assay were compared with a linear calibration curve. All assays were performed by a trained scientist (S.Y. and R.S.).

The enrolled MD patients were clinically evaluated for disease severity using two rating systems: the Japanese Mitochondrial Disease Rating Scale (JMDRS)[9] and the Newcastle Mitochondrial Disease Rating Scale (NMDAS).[10] All scores were also evaluated with respect to the levels of GDF-15 or FGF-21 using correlation coefficients.

Statistical Analysis

The diagnostic test for MD using GDF-15 was evaluated by receive operating characteristic (ROC) curve analyses. The threshold value was determined using the Youden index. Ninety-five percent confidence intervals (95% CIs) for the area

TABLE 2. JMDRS and NMDAS Scores for Each Mitochondrial Disorder

	N	JMDRS	Range	NMDAS	Range
MELAS	12	30.3 ± 17.7	4–60	36.0 ± 2 3.4	8–82
MELA	11	9.9 ± 9.4	0–27	12.6 ± 8.3	0–24
KSS	3	26.0 ± 18.4	5–39	45.7 ± 18.9	25–62
Overlapping MELAS/LS	2	15.0 ± 7.1	10–20	48.5 ± 10.1	41–56
LS	3	67.0 ± 15.7	56–85	94.7 ± 19.9	72–103

JMDRS = Japanese Mitochondrial Disease Rating Scale; KSS = Kearns-Sayre syndrome; LS = Leigh syndrome; MELA = mitochondrial encephalopathy, lactic acidosis (mitochondrial myopathy); MELAS = mitochondrial encephalopathy, lactic acidosis, and stroke-like episodes; NMDAS = Newcastle Mitochondrial Disease Rating Scale.

under the curve (AUC) of the ROC were obtained. Leave-one-out cross-validation of GDF-15 and FGF-21 was performed. Sensitivity and specificity of GDF-15 were compared with a measurement of FGF-21 using a McNemar test. Comparison of two correlated nonparametric AUCs was also performed.[11] Spearman correlation coefficients were used to examine the associations between the biomarkers.

Role of the Funding Source

This work was supported, in part, by grant nos. 25461571 (to Y.K.), 25860891 (to S.Y.), and 25242062 (to M.T.) from the Ministry of Education, Culture, Sports, Science and Technology (MEXT) and by Grant-in-Aid no. 24-Nanchi-Ippan-005 (to Y.K.) for Research on Intractable Diseases from the Ministry of Health, Labor and Welfare of Japan.

All patients and control individuals had perceived adequate information concerning to this study according to the guidelines of the Declaration of Helsinki.

Results

We analyzed samples from 48 patients who fulfilled the clinicopathological and genetic criteria of MD. Of these 48 MD patients, 27 patients suffered from MELAS and carried the m.3243A>G mutation in mitochondrial DNA (mtDNA), with the exception of 3 patients whose

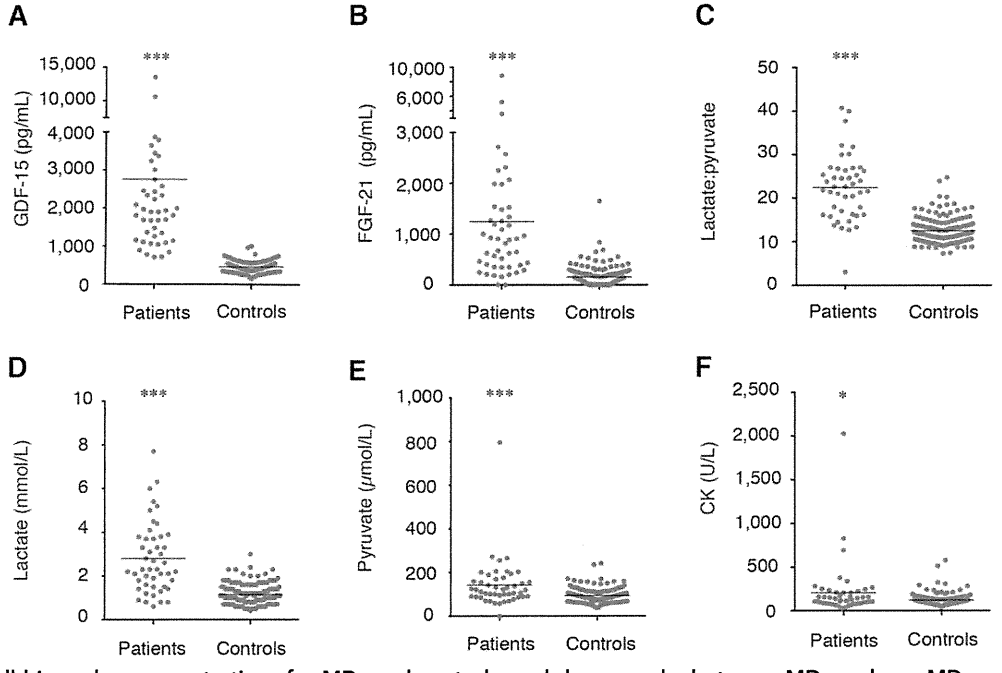

FIGURE 2: All biomarker concentrations for MDs and controls, and demography between MDs and non-MDs patients. (A) GDF-15, (B) FGF-21, (C) lactate:pyruvate ratio, (D) lactate, (E) pyruvate, and (F) CK. MD patients exhibited significantly higher levels of all biomarkers compared to controls. CK = creatine kinase; FGF-21 = fibroblast growth factor 21; GDF-15 = growth differentiation factor 15; MD = mitochondrial disorder.

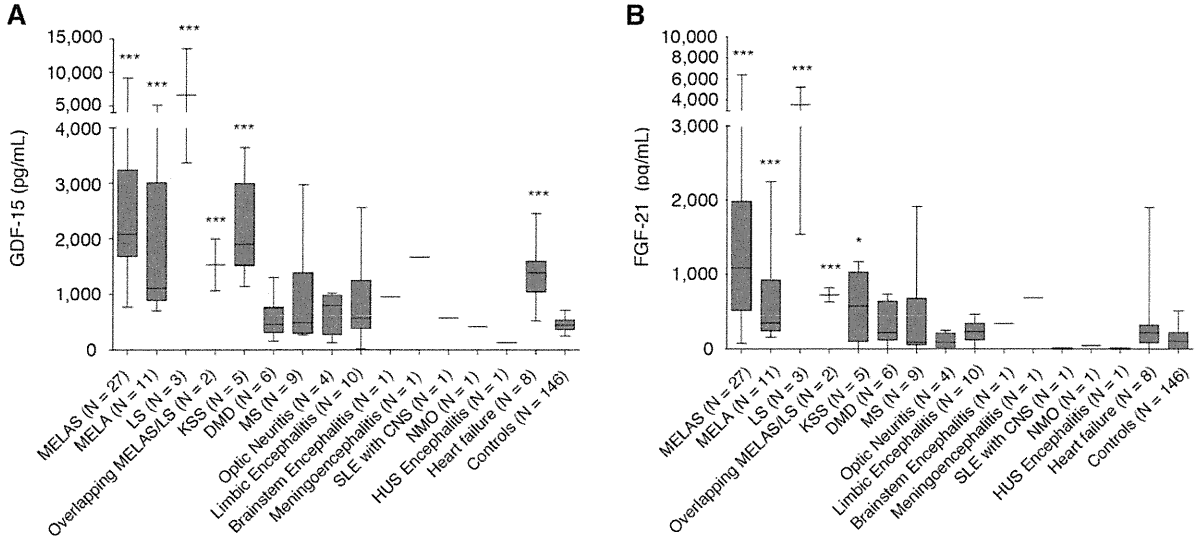

FIGURE 3: Comparison of biomarkers for MDs, and GDF-15 and FGF-21 concentrations for MDs and non-MDs. GDF-15 and FGF-21 concentrations in the patients who suffered from MD subtypes, DMD, MS, optic neuritis, limbic encephalitis, brainstem encephalitis, menigoencephalitis, SLE with CNS, NMO, and HUS encephalitis, and HF, and the control group are shown. Each MD subtype displayed significantly higher levels of GDF-15 and FGF-21 than the control group. HF displayed significantly higher levels of only GDF-15 than the control group. (A) GDF-15 and (B) FGF-21. CNS = central nervous system; DMD = Duchenne muscular dystrophy; FGF-21 = fibroblast growth factor 21; GDF-15 = growth differentiation factor 15; HUS = hemolytic uremic syndrome; KSS = Kearns-Sayre syndrome; LS = Leigh syndrome; MD = mitochondrial disorder; MS = multiple sclerosis; MELA = mitochondrial encephalopathy, lactic acidosis (mitochondrial myopathy); MELAS = mitochondrial encephalopathy, lactic acidosis, and stroke-like episodes; NMO = neuromyelitis optica; SLE = systemic lupus erythematosus.

molecular defects had not been identified. Eleven patients suffered from MELA and carried the m.3243A>G mutation. Three patients were diagnosed as LS, including 1 patient who exhibited a cytochrome *c* oxidase deficiency, 1 patient who carried the m.3243A>G mutation, and 1 patient who carried the m.8993T>C mutation. Two patients suffered from overlapping MELAS/LS and carried the m.3243A>G mutation, and 5 patients suffered from KSS and carried a common large deletion in mtDNA. The demographic characteristics of the patients in this study are shown in Table 1. We also recruited 149 healthy controls; however, 3 individuals were excluded because of abnormal thyroid function (Fig. 1B).

We evaluated the severity of each patient using two rating systems, the JMDRS[9] and the NMDAS,[10] as shown in Supplementary Table 1. The JMDRS has been used in a Japanese MELAS cohort study and has been demonstrated to be useful for the evaluation of disease progression at 5-year intervals.[9] Mean scores of MD patients on the JMDRS and the NMDAS are shown in Table 2.

The concentrations of GDF-15 and FGF-21 did not differ by age, sex, or diurnal variation.[12] The mean concentration of GDF-15 and FGF-21 is shown in Supplementary Table 2. The concentration range of GDF-15 in the MD patients was substantially higher compared to the controls. GDF-15 concentration did not overlap between MD patients and controls; however, FGF-21 concentration occasionally overlapped. In contrast, the GDF-15 reference range in healthy controls was markedly narrow, as shown in Figure 2. GDF-15 concentration was higher in HF patients compared to controls; however, FGF-21 was not different between the HF patients and controls. GDF-15 and FGF-21 concentrations were not significantly different between the DMD, the MS, optic neuritis, limbic encephalitis patients, and controls (Fig 3).

Among the various MD subtypes, GDF-15 and FGF-21 concentrations were the highest in LS and were 10-fold higher than controls. GDF-15 and FGF-21 concentrations in MELAS and MELA patients displayed broad distributions. GDF-15 and FGF-21 concentrations in KSS patients tended to be lower compared to LS, MELAS, and MELA patients; however, they were significantly higher than the controls (Supplementary Table 2).

The correlation coefficients between the concentrations of GDF-15 and FGF-21 and the JMDRS and NMDAS were positively correlated (GDF-15: $r = 0.76$ [$p < 0.001$] for the JMDRS and $r = 0.67$ [$p < 0.001$]

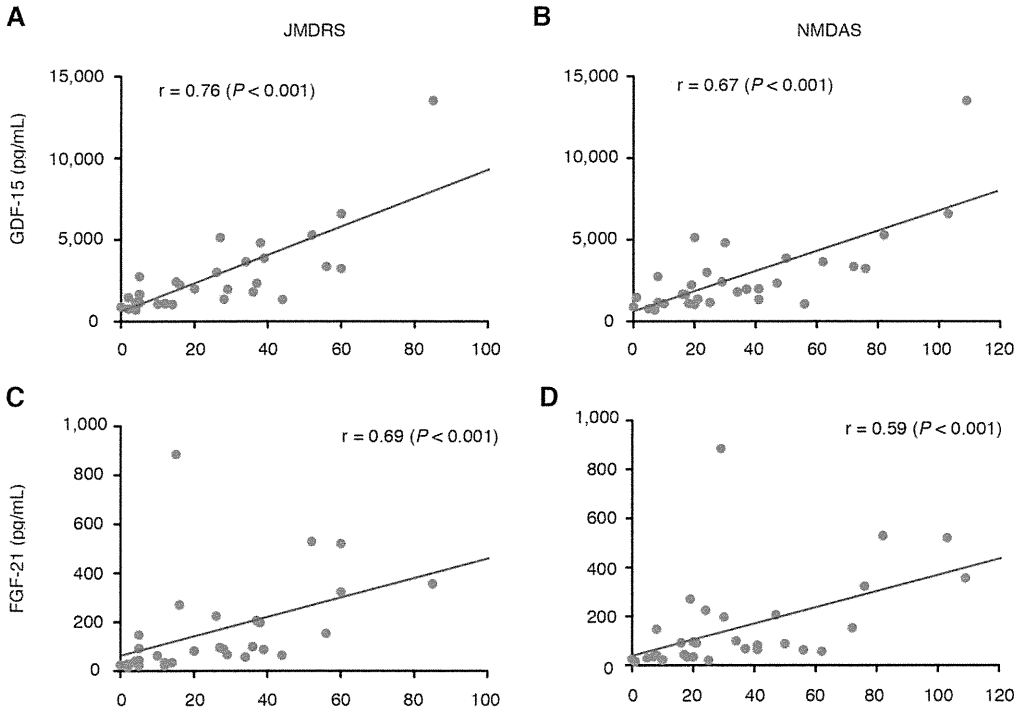

FIGURE 4: Correlation coefficients between levels of GDF-15 and FGF-21 and the JMDRS and NMDAS. GDF-15 and FGF-21 levels were positively correlated with the JMDRS and NMDAS: GDF-15: r = 0.76 (A: $p < 0.001$) for the JMDRS and r = 0.67 (B: $p < 0.001$) for the NMDAS; FGF-21: r = 0.69 (C: $p < 0.001$) for the JMDRS and r = 0.59 (D: $p < 0.001$) for the NMDAS. Spearman correlation coefficients were calculated for the statistical analysis. FGF-21 = fibroblast growth factor 21; GDF-15 = growth differentiation factor 15; JMDRS = Japanese Mitochondrial Disease Rating Scale; KSS = Kearns-Sayre syndrome; LS = Leigh syndrome; MELA = mitochondrial encephalopathy, lactic acidosis (mitochondrial myopathy); NMDAS = Newcastle Mitochondrial Disease Adult Scale.

for the NMDAS; FGF-21: r = 0.69 [$p < 0.001$] for the JMDRS and r = 0.59 [$p < 0.001$] for the NMDAS), as shown in Figure 4. The concentration of GDF-15 and FGF-21 were positively correlated (r = 0.64; $p < 0.001$), as shown in Figure 5.

AUC analyses indicated that the sensitivity and specificity were significantly larger for GDF-15 than those for FGF-21, lactate, pyruvate, the L/P ratio, or CK. The AUC was 0.997 (95% CI: 0.993–1.000) for GDF-15, 0.889 (95% CI: 0.837–0.962) for FGF-21,

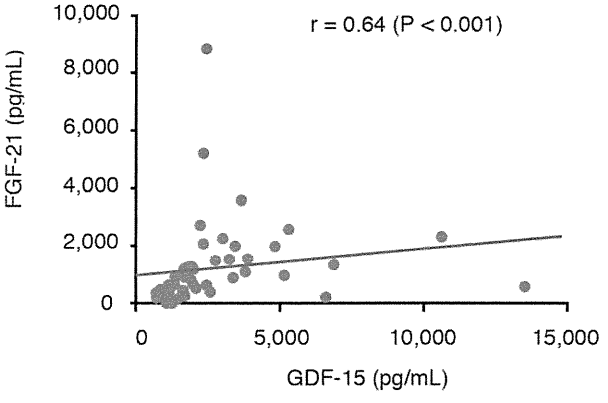

FIGURE 5: Correlation between GDF-15 and FGF-21 for MDs. GDF-15 and FGF-21 levels were positively correlated for mitochondrial disorders (MDs): r = 0.64 ($p < 0.001$). Spearman correlation coefficients were calculated for the statistical analysis. FGF-21 = fibroblast growth factor 21; GDF-15 = growth differentiation factor 15.

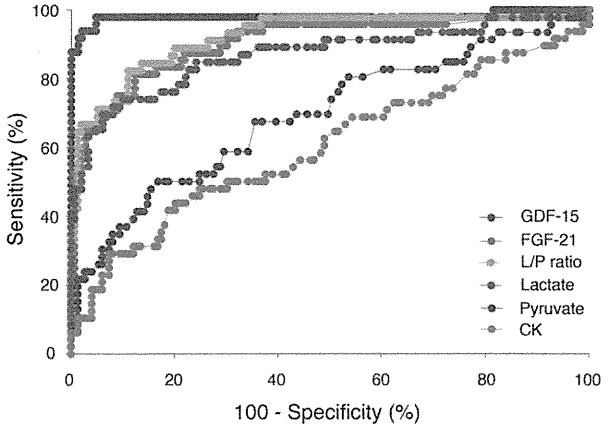

FIGURE 6: ROC curves for each biomarker in the MD patients. AUC values were 0.997 (95% confidence interval [CI]: 0.993–1.000) for GDF-15, 0.919 (95% CI: 0.865–0.973) for the lactate-to-pyruvate ratio, 0.889 (95% CI: 0.837–0.962) for FGF-21, 0.882 (95% CI: 0.814–0.950) for lactate, 0.706 (95% CI: 0.614–0.798) for pyruvate, and 0.609 (95% CI: 0.506–0.711) for creatine kinase (CK). AUC = area under the curve; FGF-21 = fibroblast growth factor 21; GDF-15 = growth differentiation factor 15; L/P ratio = lactate-to-pyruvate ratio; MD = mitochondrial disorder; ROC = receiver operating characteristic.

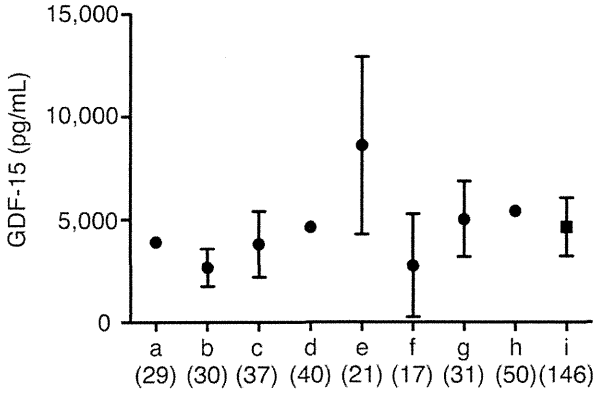

FIGURE 7: GDF-15 concentrations in the healthy controls reported from literatures. GDF-15 concentrations were recruited from literatures measured by the same ELISA kit (R&D Systems, Minneapolis, MN), that are a[13], b[14], c[8], d[15], e[16], f[17], g[18], h[19], and i (our data). Data are shown in mean ± standard deviation (SD). References of a[13], d[15], and h[19] are not described in SD. The number in parenthesis shows sample number. Our GDF-15 level in the healthy controls was similar to previous literatures.[8,13–19] GDF-15 = growth differentiation factor 15.

0.919 (95% CI: 0.865–0.973) for the L/P ratio, 0.882 (95% CI: 0.814–0.950) for lactate, 0.706 (95% CI: 0.614–0.798) for pyruvate, and 0.609 (95% CI: 0.506–0.711) for CK (Fig 6). Two correlated nonparametric AUCs were compared based on statistical analysis.[11] AUC for GDF-15 (0.997; standard error [SE] = 0.002) was significantly larger (p = 0.002) than in FGF-21 (0.899; SE = 0.032) (difference: 0.098; Z-test: 3.07; $Pr > |Z|$: 0.002).

Based on our statistical analysis, we identified a threshold value of 710.0 pg/mL GDF-15 to diagnose MDs. For FGF-21, we also identified a threshold value of 350.0 pg/mL FGF-21 to diagnose MDs. The threshold values for each biomarker were defined based on the central laboratory results as follows: 1.9 mmol/L lactate, 106.8 μmol/L pyruvate, L/P ratio of 30, and CK depending on the age group, as described in Supplementary Table 3. We identified a distribution of abnormal values of those biomarkers. Based on this analysis, sensitivities of GDF-15 and FGF-21 were 97.9% and 77.1%, respectively (p = 0.0063) and specificities of GDF-15 and FGF-21 were 95.2% and 87.7%, respectively (p = 0.0266). We tested cross-validation for GDF-15 and FGF-21. The cross-validated sensitivity and 1-specificity for both biomarkers (N = 194) were the following: The error rates (proportion of incorrectly classified sample) of GDF-15 were 4.6 ± 21.1% and FGF-21 was 14.9 ± 35.7%.

The mean level and range of GDF-15 in the controls are shown in Figure 7: a: 390 (SD not described; N = 29) pg/mL[13]; b: 267 ± 91.2 (N = 30) pg/mL[14]; c: 380.5 ± 160 (N = 37) pg/mL[8]; d: 463 (SD not described; N = 40) pg/mL[15]; e: 858.98 ± 431.45 (N = 21) pg/mL[16]; f: 276 ± 251 (N = 17) pg/mL[17]; g: 501 ± 183 (N = 31) pg/mL[18]; h: 540.09 (SD not described; N = 50) pg/mL.[19] Our data of the mean level and range of GDF-15 show as i: 462.5 ± 141.0 (N = 146) pg/mL.

The ID number, mean age, mean BMI, and % males for the controls, MD patients, and disease controls are presented in Table 1 and Supplementary Table 1.

Discussion

In this study, we have shown that GDF-15 appears to serve as a sensitive and specific biomarker for the diagnosis and/or the monitoring of disease progression of MDs in adults and children. GDF-15 exhibited greater sensitivity and specificity than FGF-21. FGF-21 has been reported to be a useful biomarker for muscle-manifesting MDs[3]; however, there were many overlapping values between controls and MD patients in our data. Because a moderate increase in FGF-21 concentration has been reported in a cachexic child with progeria,[3] further investigation is required to investigate the specific conditions that induce FGF-21 secretion. GDF-15 has also been reported to be a useful biomarker for monitoring the state of HF, renal failure, and certain cancers. The confounding factors that modulate the concentrations of GDF-15 and FGF-21 remain to be identified. When non-MD patients were complicated with HF and/or renal failure, the concentration of GDF-15 was elevated in the range of lower values of those observed in MD patients without heart and/or renal failure. However, we can distinguish easily between non-MD patients with HF and/or renal failure, and MDs without those complication, by the information of clinical findings and laboratory data, such as creatinine, blood urea nitrogen, and brain natriuretic peptide. On the other hand, diseases for similar clinical manifestations with MDs, such as DMD, MS, optic neuritis, and limbic encephalitis, are often difficult to distinguish from MDs even using routine laboratory data. In these clinical conditions, we believe that we can distinguish MD patients from patients with MD-like symptoms by evaluation of GDF-15.

In general, LS is clinically recognized as the most severe phenotype of the MD subtypes examined in this study because LS patients typically die before 10 years of age. According to both scaling system scores, LS displayed the highest scores of all examined MD subtypes. The mean level of GDF-15 in LS patients was the highest of all MD patients. All LS patients in this study were in a bed-ridden state, whereas the clinically diagnosed MELAS patients exhibited a variety of disease severities

that ranged from normal function, easy fatigability, severe myopathy with sensorineural hearing loss, and diabetes mellitus to bed-ridden (terminal stage). On the other hand, we believe that MELA and KSS patients typically maintain normal or subnormal states with respect to the activities of daily living compared with LS and MELAS patients.

The correlations between the JMDRS and NMDAS scores and the GDF-15 and FGF-21 concentrations are shown in Figure 4. The scores according to both scale systems were the highest for LS; these scores are strongly influenced by clinical severity, and LS displayed the most severe phenotype in our study. The LS patients in our study were bed-ridden and tube-fed. In contrast, the scores for MELAS patients were highly variable for both scales and were lower than those for LS, but higher than those for KSS and MELA. The clinical scores of MELAS Patients 17 and 18, who were in the bed-ridden stage, were high on both the JMDRS and the NMDAS, which is consistent with the levels of GDF-15 and FGF-21. The overlapping MELAS/LS patients displayed highly variable scores among individuals. Thus, GDF-15 and FGF-21 may serve as quantitative biomarkers.

These results demonstrate that GDF-15 is the most useful biomarker for MDs compared with FGF-21, lactate, pyruvate, the L/P ratio, and CK. GDF-15 may serve as a useful tool to quantitatively monitor disease severity of our indexed MD subtypes.

GDF-15 is a more useful biomarker for muscle-related MDs because of its substantially higher sensitivity and specificity than FGF-21 and other conventional biomarkers. FGF-21 was the best biomarker for muscle-manifested MDs, as reported in 2011.[3] We originally used FGF-21 as a primary screening test for MDs; however, it was occasionally difficult to distinguish MD patients from non-MD individuals based on FGF-21 values because the reference range of FGF-21 was broad. In contrast, the reference range of GDF-15 was narrow and rarely overlapped between MD patients and non-MD individuals (Fig 2). Our reference range of GDF-15 was in accord with previous studies (Fig 7). GDF-15 may be especially useful for the diagnosis of LS and KSS because serum lactate is rarely elevated in these MDs.[1] The present results revealed that GDF-15 was significantly elevated in MD patients, which is consistent with our recent report.[6]

GDF-15 appeared to increase with the clinical severity of the MD (Fig 4). In general, MD severity is ranked in the following order: LS, overlapping MELAS/LS, MELAS, KSS, and MELA. In our study, mean GDF-15 levels were ranked in the following order: LS, MELAS, KSS, overlapping MELAS/LS, and MELA. These results suggest that GDF-15 may serve as a useful biomarker not only for the diagnosis, but also the determination of severity of MDs. GDF-15 may be potentially as useful as FGF-21 for the evaluation of drug efficacy; however, it should be verified by longitudinal studies in future.

The AUC was significantly larger for GDF-15 (0.997) compared with the conventional MD biomarkers, including FGF-21 (Fig 5). Our study demonstrated that the AUC was also larger for FGF-21 (0.889) compared with the other conventional MD biomarkers; however, the AUC was slightly larger for the L/P ratio (0.917) than for FGF-21 (0.889). The AUC for the L/P ratio (0.917) was within the 95% CI of a previous study (0.82–0.98).[3] The AUC for sFGF-21 (0.889) was not within the 95% CI of a previous study (0.94–0.99).[3] The calculated threshold values of GDF-15 and FGF-21 were 707.0 and 343.8 pg/mL, respectively. We evaluated the threshold values of 710.0 and 350.0 pg/mL for GDF-15 and FGF-21, respectively. The sensitivity and specificity of GDF-15 were 97.9% and 95.2%, respectively, and were substantially higher than FGF-21, which were 77.1% and 87.7%, respectively. Ultimately, GDF-15 was a more useful biomarker than FGF-21 whether we used our or other threshold values. The AUC was higher for FGF-21 than for the L/P ratio in a previous study[3]; however, the AUC was comparable between FGF-21 and the L/P ratio in our study. We hypothesized that these differences in the AUC for FGF-21 were because of the different MDs and ages. Our MD patients were primarily typical and classical, and the FGF-21 levels may be lower in our study than in the previous study.[3] However, the patients in the previous study were classified as MELAS, Alpers syndrome, MIRAS, and others; moreover, 26 of the 67 (38.8%) MD patients were children.[3] In our study, 12 of the 48 (25%) MD patients were children. The child MD patients exhibited higher FGF-21 levels in both our study (LS and MELAS/LS overlapping) and the previous study (Alpers syndrome and patients with mtDNA mutations).[3] Further assessment of the various MD subtypes is required.

On the other hand, GDF-15 in HF patients was significantly elevated compared to controls as well as MDs. However, FGF-21 in HF patients was not significantly elevated with controls. It is indicated that only GDF-15 does not completely distinguish HF with MDs from HF without MDs. We calculated that GDF-15 and FGF-21 were combined to analyze the severity and sensitivity for MDs, however, the severity and sensitivity in MDs were lower in combination than only GDF-15 (data not shown). Furthermore, the patients' number was too small to evaluate the severity and sensitivity.

The mechanism of elevation of GDF-15 is not clear in MDs patients. ATF4 is a master regulator of upstream of stress signals.[20] GDF-15 was upregulated by ATF4 in mouse embryonic fibroblast.[21] FGF-21 was also induced by ATF4 in mouse.[22–24] We revealed that GDF-15 and FGF-21 were elevated in MDs compared to controls, and both GDF-15 and FGF-21 levels were correlated with MDs. Therefore, we suggested that the mechanism of elevation of GDF-15 in MDs is derived from ATF4 signaling and occurred from various stresses during mitochondrial dysfunctions. More investigations are requested to clarify what kinds of interactions exist in the disease condition such as HF, kidney disease, and cancers.

In conclusion, our data suggest that the measurement of GDF-15 in combination with FGF-21 by ELISA serves as the most useful first-line test in patients with suspected MDs to prioritize patients for muscle biopsy. Using new biomarkers, we may be able to diagnose MDs at a nonspecialist hospital and reduce the unnecessary invasive biopsy procedures in children and adults.

Acknowledgment

This work was supported, in part, by grant nos. 25461571 (to Y.K.), 25860891 (to S.Y.), and 25242062 (to M.T.) from the Ministry of Education, Culture, Sports, Science and Technology (MEXT) and by Grant-in-Aid no. 24-Nanchi-Ippan-005 (to Y.K.) for Research on Intractable Diseases from the Ministry of Health, Labor and Welfare of Japan. This research is (partially) supported by the intractable/rare disorders no. 15ek0109088h0001 (to Y.K.) from Japan Agency for Medical Research and development, AMED.

We thank Dr S. Kinjo for recruiting 1 MD patient, E. Tanamachi and K. Murakami for collecting control samples, and Drs Y. Sugi and K. Mawatari for recruiting all HF patients. We also thank all patients and control individuals. We thank E. Tanamachi for technical support regarding the measurement of GDF-15 and FGF-21.

Authorship

Conception and design of the study: SY, YF, TK, MI, MT, YK. Acquisition, analysis & interpretation of data: SY, AI, YF, HA, TK, MT, RS, YK. Drafting the manuscript: SY, YF, TK, MI, MT, TK, MT, RS, YK.

Potential Conflicts of Interest

The authors declare that there is no conflict of interests regarding the publication of this paper.

Appendix

Patent

M.T., Y.F., M.I., and Y.K. have a patent PCT/JP2015/50833 issued. A patent is pending for the usefulness of GDF-15 for the biomarker of mitochondrial disorders. Patent rights are assigned to the Tokyo Metropolitan Institute of Gerontology and Kurume University.

References

1. Haas RH, Parikh S, Falk MJ, et al. Mitochondrial disease: a practical approach for primary care physicians. Pediatrics 2007;120:1326–1333.
2. Munnich A, Rotig A, Chretien D, et al. Clinical presentation of mitochondrial disorders in childhood. J Inherit Metab Dis 1996;19:521–527.
3. Suomalainen A, Elo JM, Pietiläinen KH, et al. FGF-21 as a biomarker for muscle-manifesting mitochondrial respiratory chain deficiencies: a diagnostic study. Lancet Neurol 2011;10:806–818.
4. Davis RL, Liang C, Edema-Hildebrand F, et al. Fibroblast growth factor 21 is a sensitive biomarker of mitochondrial disease. Neurology 2013;81:1819–1826.
5. Liang C, Ahmad K, Sue CM. The broadening spectrum of mitochondrial disease: shifts in the diagnostic paradigm. Biochim Biophys Acta 2014;1840:1360–1367.
6. Fujita Y, Ito M, Kojima T, et al. GDF15 is a novel biomarker to evaluate efficacy of pyruvate therapy for mitochondrial diseases. Mitochondrion 2014;20:34–42.
7. Lindahl B. The story of growth differentiation factor 15: another piece of the puzzle. Clin Chem 2013;59:1550–1552.
8. Kalko SG, Paco S, Jou C, et al. Transcriptomic profiling of TK2 deficient human skeletal muscle suggests a role for the p53 signalling pathway and identifies growth and differentiation factor-15 as a potential novel biomarker for mitochondrial myopathies. BMC Genomics 2014;15:91.
9. Yatsuga S, Povalko N, Nishioka J, et al. MELAS: a nationwide prospective cohort study of 96 patients in Japan. Biochim Biophys Acta 2012;1820:619–624.
10. Schaefer AM, Phoenix C, Elson JL, et al. Mitochondrial disease in adults: a scale to monitor progression and treatment. Neurology 2006;66:1932–1934.
11. Delong ER, Delong DM, Clarke-Pearson DL. Comparing the area under two or more correlated receiver operating characteristic curves: a non parametric approach. Biometrics. 1988;44:837–845.
12. Cantó C, Auwerx J. FGF21 takes a fat bite. Science 2012;336:675–676.
13. Lambrecht S, Smith V, De Wilde K, et al. Growth differentiation factor 15, a marker of lung involvement in systemic sclerosis, is involved in fibrosis development but is not indispensable for fibrosis development. Arthritis Rheumatol 2014;66:418–427.
14. Yang CZ, Ma J, Luo QQ, et al. Elevated level of serum growth differentiation factor 15 is associated with oral leukoplakia and oral squamous cell carcinoma. J Oral Pathol Med 2014;43:28–34.
15. Cui R, Gale RP, Zhu G, et al. Serum iron metabolism and erythropoiesis in patients with myelodysplastic syndrome not receiving RBC transfusions. Leuk Res 2014;38:545–550.
16. Tarkun P, Mehtap O, Atesoglu EB, et al. Serum hepcidin and growth differentiation factor-15 (GDF-15) levels in polycythemia vera and essential thrombocythemia. Eur J Haematol 2013;91:228–235.
17. Shalev H, Phillip M, Galil A, et al. High levels of soluble serum hemojuvelin in patients with congenital dyserythropoietic anemia type I. Eur J Haematol 2013;90:31–36.

18. Schiegnitz E, Kammerer PW, Koch FP, et al. GDF 15 as an anti-apoptotic, diagnostic and prognostic marker in oral squamous cell carcinoma. Oral Oncol 2012;48:608–614.

19. Santhanakrishnan R, Chong JPC, Ng TP, et al. Growth differentiation factor 15, ST2, high-sensitivity troponin T, and N-terminal pro brain natriuretic peptide in heart failure with preserved vs. reduced ejection fraction. Eur J Heart Fail 2012; 14:1338–1347.

20. Harding HP, Zhang Y. Zeng H, et al. An integrated stress response regulates amino acid metabolism and resistance to oxidative stress. Mol Cell 2003;11:619–633.

21. Jousse C, Deval C, Maurin AC, et al. TRB3 inhibits the transcriptional activation of stress-regulated genes by a negative feedback on the ATF4 pathway. J Biol Chem 2007;282:15851–15861.

22. De Sousa-Coelho AL, Marrero PF. Haro D. Activating transcription factor 4-dependent induction of FGF21 during amino acid deprivation. Biochem J 2012;443:165–171.

23. Jiang S, Yan C. Fang QC, et al. Fibroblast growth factor 21 is regulated by the IRE1α-XBP1 branch of the unfolded protein response and counteracts endoplasmic reticulum stress-induced hepatic steatosis. J Biol Chem 2014;289:29751–29765.

24. Kim KH, Jeong YT, Kim SH, et al. Metformin-induced inhibition of the mitochondrial respiratory chain increases FGF21 expression via ATF4 activation. Biochem Biophys Res Commun 2013;440: 76–81.

Human Molecular Genetics, 2015, Vol. 24, No. 10 2952–2965

doi: 10.1093/hmg/ddv058
Advance Access Publication Date: 12 February 2015
Original Article

ORIGINAL ARTICLE

Characterization of mitochondrial FOXRED1 in the assembly of respiratory chain complex I

Luke E. Formosa[1,2,†], Masakazu Mimaki[1,‡,†], Ann E. Frazier[3], Matthew McKenzie[4], Tegan L. Stait[3], David R. Thorburn[3,5], David A. Stroud[2] and Michael T. Ryan[2,*]

[1]Department of Biochemistry, La Trobe Institute for Molecular Science, La Trobe University, Melbourne, VIC 3086, Australia, [2]Department of Biochemistry and Molecular Biology, Monash University, Clayton, Melbourne 3800, Australia, [3]Murdoch Childrens Research Institute, Royal Children's Hospital and University of Melbourne Department of Paediatrics, University of Melbourne, Melbourne, VIC 3052, Australia, [4]Centre for Genetic Diseases, MIMR-PHI Institute of Medical Research, Clayton, Melbourne 3168, Australia and [5]Victorian Clinical Genetics Services, Royal Children's Hospital, Melbourne, VIC 3052, Australia

*To whom correspondence should be addressed. Email: Michael.Ryan@monash.edu

Abstract

Human mitochondrial complex I is the largest enzyme of the respiratory chain and is composed of 44 different subunits. Complex I subunits are encoded by both nuclear and mitochondrial (mt) DNA and their assembly requires a number of additional proteins. FAD-dependent oxidoreductase domain-containing protein 1 (FOXRED1) was recently identified as a putative assembly factor and *FOXRED1* mutations in patients cause complex I deficiency; however, its role in assembly is unknown. Here, we demonstrate that FOXRED1 is involved in mid-late stages of complex I assembly. In a patient with *FOXRED1* mutations, the levels of mature complex I were markedly decreased, and a smaller ~475 kDa subcomplex was detected. In the absence of FOXRED1, mtDNA-encoded complex I subunits are still translated and transiently assembled into a late stage ~815 kDa intermediate; but instead of transitioning further to the mature complex I, the intermediate breaks down to an ~475 kDa complex. As the patient cells contained residual assembled complex I, we disrupted the *FOXRED1* gene in HEK293T cells through TALEN-mediated gene editing. Cells lacking FOXRED1 had ~10% complex I levels, reduced complex I activity, and were unable to grow on galactose media. Interestingly, overexpression of FOXRED1 containing the patient mutations was able to rescue complex I assembly. In addition, FOXRED1 was found to co-immunoprecipitate with a number of complex I subunits. Our studies reveal that FOXRED1 is a crucial component in the productive assembly of complex I and that mutations in *FOXRED1* leading to partial loss of function cause defects in complex I biogenesis.

Introduction

Mitochondrial complex I (NADH:ubiquinone oxidoreductase) is the largest complex of the mitochondrial respiratory chain (1). It is located in the mitochondrial inner membrane and protrudes into the matrix to form an L-shaped structure (2) and also assembles with other respiratory chain complexes to form respirasomes (3). Isolated defects in complex I are the most common of the mitochondrial respiratory chain disorders (4,5) and complex I dysfunction has also been implicated in Parkinson's disease (6,7) and aging (8). In humans, complex I consists of 44

† These authors contributed equally.
‡ Present address: Department of Pediatrics, Teikyo University School of Medicine, Tokyo, Japan.
Received: November 4, 2014. **Revised:** January 14, 2015. **Accepted:** February 9, 2015

different subunits (9–11), with one subunit located at two separate sites (2). Seven subunits, ND1–ND6 and ND4L, are encoded by mitochondrial DNA (mtDNA) and are found in the membrane arm or proton translocation module (P module). The remaining 37 subunits are encoded by nuclear DNA (nDNA) and imported into the mitochondria (12–14). Seven of the nDNA-encoded subunits (NDUFV1, NDUFV2, NDUFS1, NDUFS2, NDUFS3, NDUFS7 and NDUFS8) are 'core subunits' of the peripheral, or matrix, arm of complex I, catalyzing the oxidation of NADH (at the N module) and electron transfer (at the Q module) to ubiquinone (15,16). The remaining 30 nDNA-encoded subunits are referred to as 'accessory' subunits, and are proposed to assist in complex I biogenesis and support the structural stability of the enzyme (9,12,17). The recent structural characterization of the bovine enzyme supports this concept (2).

Complex I assembly is proposed to involve a stepwise process with intermediate complexes shared by two assembly pathways: *de novo* synthesis headed by mtDNA-encoded subunits and the dynamic exchange of newly imported nDNA-encoded subunits with pre-existing components of the mature complex (18–20). The complicated assembly of such a large number of subunits into the mature holocomplex I requires a number of assembly factors that are not part of the final structure of complex I. To date, at least 12 known or putative complex I assembly factors have been described and mutations in 9 of these are associated with isolated complex I deficiency due to impaired complex I biogenesis (19,21–23).

While defects in assembly cause mitochondrial disease, it was recently reported that efficient assembly of complex I is also associated with longevity in mice (8). It is therefore important to understand the intricacies of the assembly pathway to determine potential therapeutic approaches to combat disease and aging. Phylogenetic profiling and subsequent knockdown studies identified FOXRED1 as a candidate protein for complex I biogenesis (24). Two separate studies subsequently found that mutations in *FOXRED1* cause complex I deficiency and mitochondrial disease (25,26). However, it is thus far not known how FOXRED1 functions in complex I biogenesis. Here, we demonstrate that FOXRED1 acts as a crucial factor in the productive assembly of complex I intermediates and that patient mutations represent partial loss of function that can be overcome by overexpression.

Results

FOXRED1 is associated with the matrix face of the mitochondrial inner membrane

FOXRED1 is a 54 kDa protein with a putative FAD-binding site and lacking a predicted transmembrane anchor. It was suggested that FOXRED1 may contain a cleavable mitochondrial targeting signal (26), but this has not been biochemically addressed. *In vitro* import analysis was conducted where radiolabeled FOXRED1 was incubated with isolated mitochondria for various times, and import monitored by SDS–PAGE (27). FOXRED1 migrated at its predicted size of 54 kDa (Fig. 1A, lane 1). After incubation with mitochondria for various times, the size of FOXRED1 did not alter, although it was protected from externally added proteinase K, indicating that like a subset of matrix-directed proteins (28,29), FOXRED1 lacks a cleavable targeting signal. Furthermore, like other proteins imported into the inner membrane or matrix (30), FOXRED1 import was dependent on the presence of a mitochondrial membrane potential ($\Delta\Psi_m$; Fig. 1A, lane 9).

To confirm the sub-mitochondrial location of FOXRED1, we expressed a C-terminal FLAG-tagged construct of FOXRED1 in

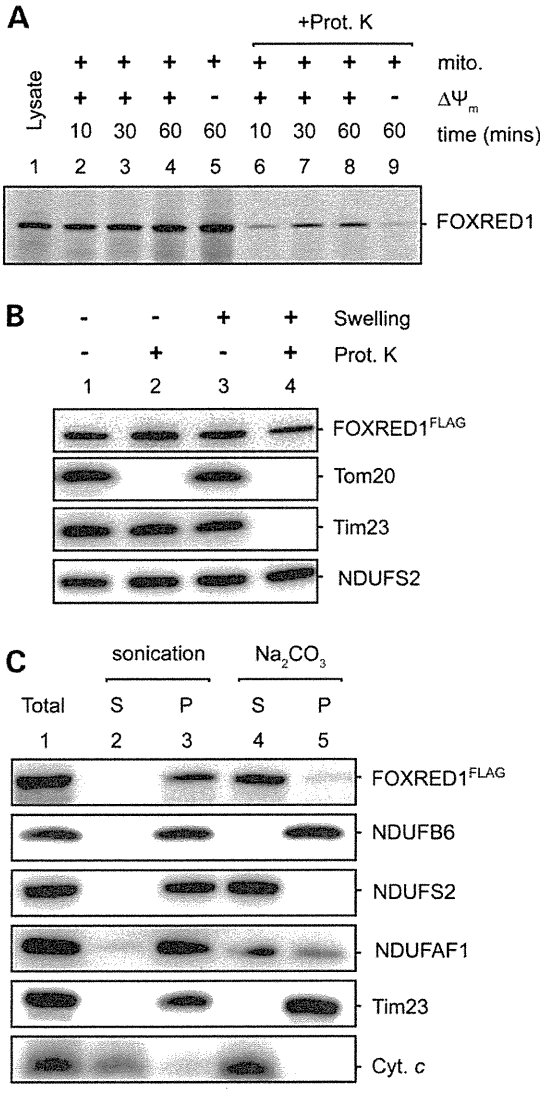

Figure 1. Mitochondrial localization of FOXRED1. (**A**) Radiolabeled FOXRED1 was incubated for various times (10–60 min) with mitochondria isolated from HEK293T cells in the presence or absence of a membrane potential ($\Delta\Psi_m$). Samples were treated with or without proteinase K (Prot. K) and were subjected to SDS–PAGE and phosphorimage analysis. (**B**) Mitochondria were isolated from HEK293T cells expressing FOXRED1^{FLAG}, followed by outer membrane rupture (swelling) and treatment with Prot. K. Samples were subjected to SDS–PAGE and western blot analysis. The proteins Tim23 and Tom20 served as controls for an inner membrane protein facing the intermembrane space and an outer membrane protein, respectively. The protein NDUFS2 was used as a control for matrix localization. (**C**) Mitochondria were isolated from HEK293T cells expressing FOXRED1^{FLAG} and subjected to sonication or sodium carbonate (Na_2CO_3) treatment. After ultracentrifugation, supernatant (S) and pellet (P) fractions were subjected to SDS–PAGE and western blot analysis. Total indicates the mitochondria without any treatment. Antibodies against NDUFB6 and Tim23 were used as controls for integral membrane proteins, NDUFS2 and NDUFAF1 were used as peripheral membrane proteins and cytochrome *c* (Cyt. *c*) as a soluble intermembrane space protein.

HEK293T cells. Mitochondria were isolated and incubated in a low-sucrose concentration buffer to induce outer membrane rupture, followed by treatment with exogenous proteinase K (27). FOXRED1 was detected as a protease-resistant protein, suggesting that it was facing the mitochondrial matrix (Fig. 1B, lane 4). As controls, the outer membrane protein Tom20 was degraded by protease treatment both before and after outer membrane rupture (Fig. 1B, lanes 2 and 4), while Tim23, an inner membrane

protein that faces the intermembrane space of the inner membrane, was initially protected from protease treatment (Fig. 1B, lane 2), but was degraded following outer membrane rupture (Fig. 1B, lane 4). Additionally, the complex I subunit NDUFS2, which is located in the mitochondrial matrix, was protected from protease treatment after outer membrane rupture (Fig. 1B, lane 4). In order to determine whether FOXRED1 associates with the inner membrane, mitochondria were isolated from HEK293T cells transfected with the FOXRED1^{FLAG} construct and either sonicated or subjected to alkaline extraction with sodium carbonate (27). FOXRED1 was found in the pellet but not the supernatant fraction after sonication, indicating its membrane association (Fig. 1C, lanes 2 and 3). After alkaline extraction, FOXRED1 was found in the supernatant but not the pellet (Fig. 1C, lanes 4 and 5), suggesting that it peripherally associates with the inner membrane. The membrane arm complex I subunit NDUFB6 and the matrix arm complex I subunit NDUFS2 were used as controls for integral and peripheral membrane proteins, respectively. The complex I assembly factor, NDUFAF1 (CIA30), which peripherally associates with the inner membrane (31), was also detected in the pellet after sonication, and largely released into the supernatant after sodium carbonate treatment (Fig. 1C, lanes 3 and 4). As expected, Tim23 was found in the pellet after both sonication and carbonate extraction (Fig. 1C, lanes 3 and 5) while cytochrome c was found in the soluble fraction (Fig. 1C, lanes 2 and 4). The combined import and immunoblot results indicate that FOXRED1 resides on the matrix face of the inner membrane, consistent with its role in complex I biogenesis.

FOXRED1 patient cells have reduced complex I and accumulate an ~475 kDa subcomplex that is rescued upon complementation

Compound heterozygous mutations in the *FOXRED1* gene were identified in a patient with Leigh syndrome showing isolated complex I deficiency (25). The two mutations in the *FOXRED1* gene were a c.694C > T transition resulting in a Gln232 to premature stop alteration (p.Q232*) and a 1289A > G transition resulting in an Asn430 to Ser change (p.N430S).

As we have found significant variability in oxygen consumption between different control fibroblasts, robust differences in respiration measurements compared with patient cells is not always observed. The oxygen consumption rate (OCR) and extracellular acidification rate (ECAR) were thus determined using FOXRED1 patient fibroblasts and four different control fibroblast cell lines. As can be seen (Fig. 2A), the ECAR/OCR ratio was greater in FOXRED1 patient cells, suggesting that these cells were more reliant on glycolysis. Next we analyzed the steady-state levels of individual respiratory chain holocomplexes by solubilizing mitochondria from control and *FOXRED1* patient fibroblasts in the detergent Triton X-100 (TX), followed by BN-PAGE and western blot analysis. The amount of mature complex I in *FOXRED1* patient mitochondria was strongly reduced compared with that of control fibroblasts, whereas the levels of complexes II, III and IV appeared normal (Fig. 2B). These results are consistent with the diagnosis of 9% residual activity of complex I in patient fibroblasts (25). Furthermore, nDNA-encoded complex I subunits NDUFS5, NDUFB6, NDUFS2, NDUFS3 and the mtDNA-encoded ND1 were decreased in patient fibroblast mitochondria compared with the control (Fig. 2C).

To investigate the assembly of complex I subunits in FOXRED1 patient mitochondria, we performed 2-dimensional BN-PAGE analysis (2D-PAGE) followed by western blot analysis using specific antibodies. All subunits tested were present in the mature complex; however, their amounts were strongly decreased in the patient mitochondria compared with the control (Fig. 2D). Interestingly, the nDNA-encoded subunit NDUFS5 and the mtDNA-encoded subunit ND1 were also observed in an ~550 kDa complex in the control. This complex represents the previously reported ~650 kDa subcomplex (19), but we now use the more accurate re-estimations of subcomplex sizes performed by Andrews and colleagues (32). In FOXRED1 patient mitochondria, these subunits were predominantly detected in a smaller complex which we refer to as being ~475 kDa. NDUFS5 has not previously been found in any detectable assembly intermediate and is thought to assemble into the holocomplex at a late stage, although a recent study suggested its presence in the ~815 kDa (previously ~830 kDa) complex that represents the mature complex lacking addition of the N-module (33). Further investigations are required to determine the entry point of this intermembrane space subunit in the CI assembly pathway. Using NDUFB6 antibodies, we detected the ~550 kDa subcomplex in both control and patient mitochondria, although the signal was weaker in the patient. In contrast to NDUFS5 and ND1, NDUFB6 was not found in the ~475 kDa subcomplex but was present in a lower form in the patient cell mitochondria. NDUFB6 is thought to assemble into an ~370 kDa (formerly ~460 kDa) intermediate along with subunits including ND2, ND3 and ND4L, although defects in assembly, including cells deficient in ND5 or ND6 lead to the appearance of NDUFB6 in smaller subcomplexes (34). NDUFS2 was also detected in lower molecular-weight subcomplexes in patient mitochondria, and similar complexes have been observed in previous studies. For example, NDUFS2 has been found in early complex I intermediates including an ~200 kDa soluble subcomplex and a 315 kDa membrane subcomplex (formerly the 400 kDa intermediate) (20). In addition, it has recently been shown that NDUFS2 is methylated at Arg85 by the assembly factor NDUFAF7 (35,36) and this stabilizes formation of the ~315 kDa intermediate that contains additional subunits including ND1. As ND1 is predominantly found at the ~475 kDa subcomplex in FOXRED1 patient cells, the NDUFS2 subcomplexes most likely represent early soluble species. This suggests that the loss of FOXRED1 likely slows the assembly process leading to the accumulation of stalled intermediates.

In order to verify that the reduced level and assembly defects of complex I in FOXRED1 patient cells were indeed caused by a FOXRED1 deficiency, complementation analysis was performed. Expression of FOXRED1 in lentiviral transduced patient fibroblasts resulted in increased levels of mature complex I (Fig. 2E, compare lanes 2 and 3) with concomitant loss of the ~475 kDa subcomplex. In contrast, transduction of the lentiviral vector lacking FOXRED1 had no effect on complex I levels (Fig. 2E, lane 4). We conclude that the mutations in *FOXRED1* lead to reduced complex I assembly.

FOXRED1 is involved in the assembly/stability of late stage complex I intermediates

More precise assessment of complex I assembly defects can be monitored using pulse-chase assembly analysis of mtDNA-encoded subunits (37,38). Control and *FOXRED1* patient fibroblasts were pulse labeled with [^{35}S]-Met, followed by a chase of up to 24 h to enable unlabeled subunits to assemble with the radiolabelled subunits. Mitochondria were then isolated and subjected to 2D-PAGE (Fig. 3A). In control fibroblasts, the signals of mtDNA-encoded complex I subunits were observed in a characteristic ~815 kDa complex at 0 h chase (39), and after 24 h were all found in mature complex I (Fig. 3A, bottom left panel). However, while in *FOXRED1* patient fibroblasts the mtDNA-encoded

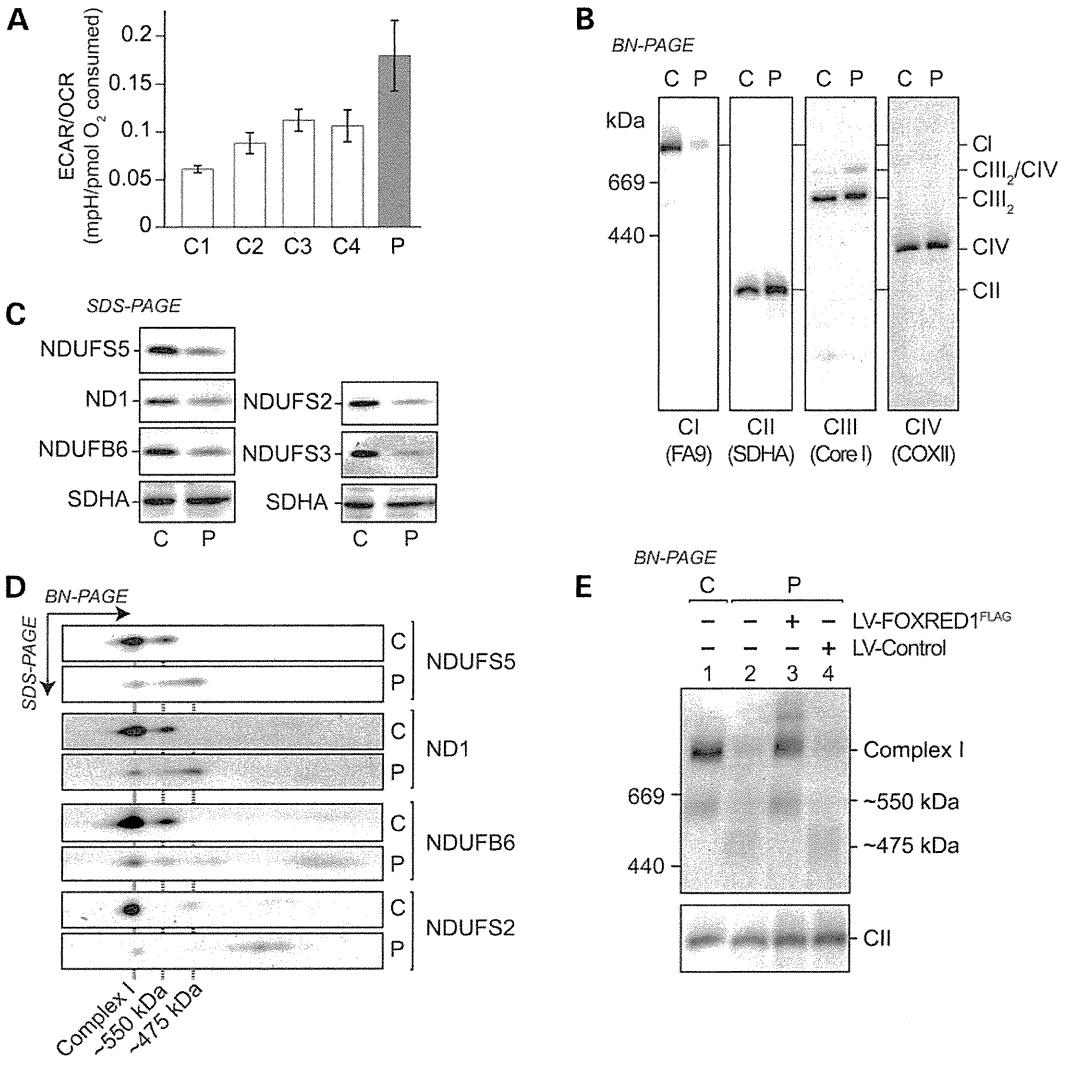

Figure 2. Complex I assembly defects in *FOXRED1* patient mitochondria. (**A**) The basal ECAR relative to basal OCR was measured in control fibroblasts (C1–C4) and FOXRED1 patient fibroblasts (P). N = 3, SEM. (**B**) Mitochondria (40 µg protein) isolated from control (C) or *FOXRED1* patient (P) fibroblasts were solubilized in 1% (v/v) TX and subjected to BN-PAGE and immunoblot analysis using antibodies against NDUFA9 (CI), SDHA (CII), Core I (CIII) and COX II (CIV). (**C**) Steady-state levels of complex I subunits in control (C) and *FOXRED1* patient (P) fibroblasts were analyzed by SDS–PAGE and western blotting using antibodies against various complex I subunits and SDHA as a loading control. (**D**) Mitochondria (100 µg protein) were isolated from control (C) or *FOXRED1* patient (P) fibroblasts, solubilized in 1% (v/v) TX and subjected to 2D BN/SDS–PAGE analysis. Immunodetection of the complex I subunits, NDUFS5, ND1, NDUFB6 and NDUFS2, was performed. (**E**) *FOXRED1* patient fibroblasts were transduced with lentiviral (LV) empty vector (LV-Control) or expressing wild-type FOXRED1. Mitochondria were isolated and solubilized in 1% TX for BN-PAGE followed by western blot analysis. Untreated control (C) and FOXRED1 patient fibroblasts (P) were also analyzed as controls. Antibodies against NDUFS5 and SDHA were used to detect complex I (CI) and complex II (CII; loading control), respectively.

subunits assembled into the ~815 kDa complex following labeling (0 h chase), they did not subsequently assemble into the mature complex and were detected in a smaller ~475 kDa complex (Fig. 3A, right).

The complex I assembly factor NDUFAF1 (CIA30), along with other assembly factors, associates with complex I intermediates, ranging from ~315 to 815 kDa (22,31,40). To characterize the ~475 kDa complexes in *FOXRED1* patient mitochondria, we performed antibody shift assays with NDUFAF1 antibodies. After mtDNA-encoded subunit labeling, mitochondrial lysates were incubated with NDUFAF1 or pre-immune antibodies prior to 2D-PAGE (41). In order to differentiate shifted complex I subunits from other mtDNA-encoded proteins, the lane was excised and subjected to SDS–PAGE in the second dimension (Fig. 3B). In both control and *FOXRED1* patient mitochondria, complex I subunits ND1 and ND2 in the ~815 kDa were shifted with NDUFAF1 antibodies (Fig. 3B, top panels), indicating that the ~815 kDa complex in the *FOXRED1* patient mitochondria associates with NDUFAF1, like that of control fibroblast mitochondria. However, at 6 h chase where ND1 and ND2 were detected in the ~475 kDa complex in *FOXRED1* patient mitochondria, NDUFAF1 antibodies were unable to shift these subunits (Fig. 3B, bottom panels). The dissociation of NDUFAF1 suggests that the ~475 kDa complex in *FOXRED1* patient fibroblasts is not a stalled assembly intermediate but rather it represents a stable but crippled subcomplex due to defects in the late stage assembly pathway of complex I.

FOXRED1 gene disruption leads to severe complex I deficiency

Our work indicates that mutations in FOXRED1 lead to defects in the assembly of complex I. Notably, some complex I is still able to

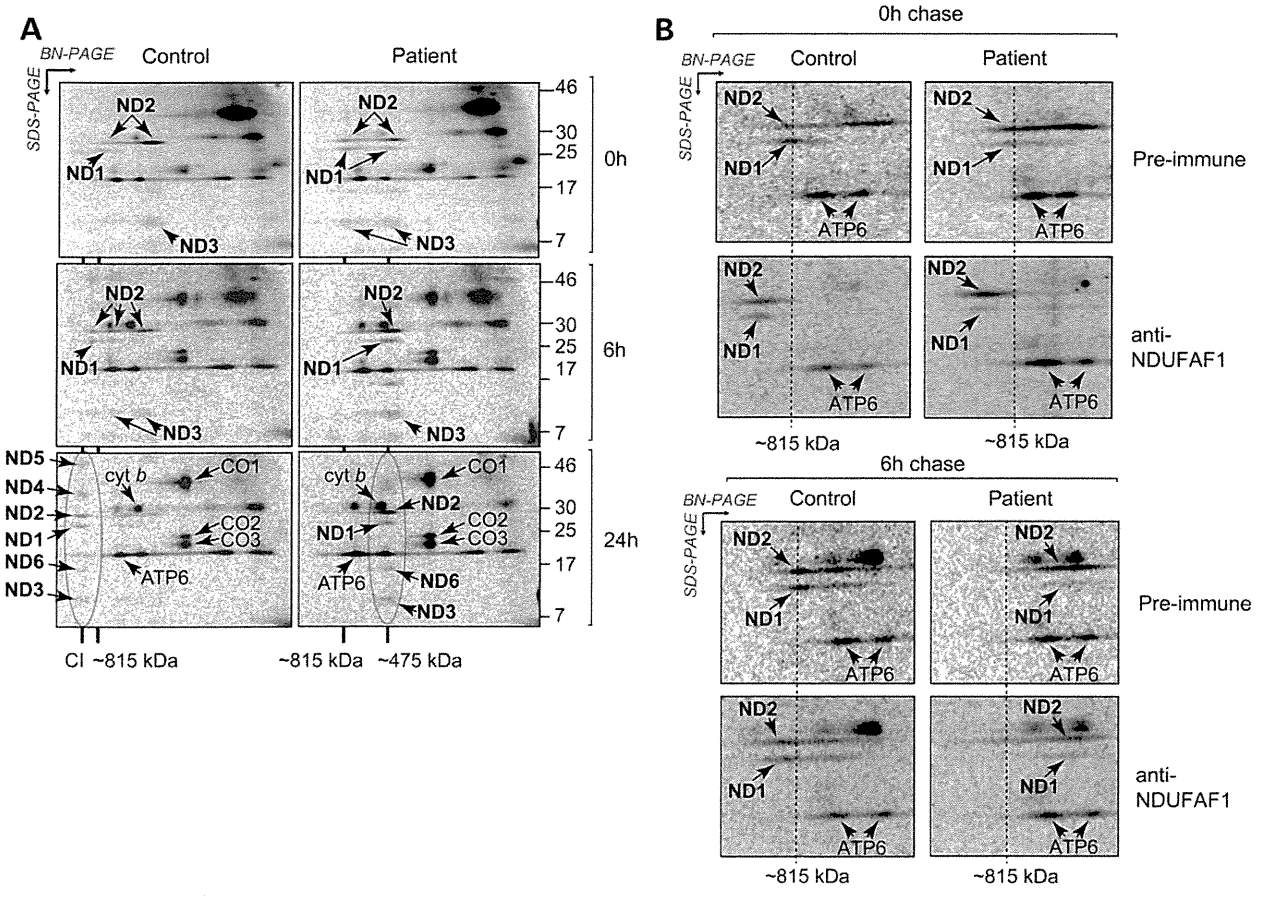

Figure 3. Analysis of complex I assembly defects in *FOXRED1* patient cells. (**A**) After radiolabeling of mtDNA-encoded subunits, control or *FOXRED1* patient fibroblasts were chased for various times (0, 6 and 24 h). Mitochondria (100 μg protein) were isolated, solubilized in 1% (v/v) TX and subjected to 2D BN/SDS–PAGE and phosphorimager analysis. The positions of subunits ND1–ND6 (complex I), cyt *b* (complex III), CO1, CO2, CO3 (complex IV) and ATP6 (complex V) are indicated. The relative position of the ~815 kDa complex, ~475 kDa complex and complex I is shown. (**B**) Antibody shift assay of radiolabelled lysates with NDUFAF1 antibodies. After radiolabeling of mtDNA-encoded subunits followed by a chase, mitochondria were isolated, solubilized in TX and incubated with NDUFAF1 antibodies or pre-immune sera. Following incubation, samples were subjected to 2D BN/SDS–PAGE analysis and phosphorimaging.

be assembled and this may explain the reason for the patients surviving into adulthood (25,26). The mutations in FOXRED1 may therefore represent a partial loss of function. To address whether FOXRED1 is absolutely necessary for complex I assembly, we used TALEN-mediated gene editing of HEK293T cells and analyzed two cell lines where expression of FOXRED1 has been disrupted (the first clone is denoted ΔFOXRED1 and the second clone, ΔFOXRED1^{C2}). We targeted the first coding exon and identified nucleotide deletions in both clones, all of which resulted in loss of the translation initiation codon (Fig. 4A). Proteomic analysis of mitochondria isolated from these cells revealed the absence of FOXRED1 peptides in comparison to control mitochondria (data not shown). In addition, both ΔFOXRED1 clones were unable to grow on media containing galactose as the sole carbon source with ~80% cell death observed after 72 h (Fig. 4B). Similar growth defects were also previously reported following gene disruption of NDUFA9 in HEK293T cells that arrested complex I assembly (33).

Western blotting with complex I subunit antibodies revealed a minor amount of assembled complex I in both the holoenzyme form (following TX solubilization) and supercomplex form (following digitonin solubilization) (Fig. 4C and D). In addition, ΔFOXRED1 mitochondria harbored NDUFS5 in an ~475 kDa complex similar to FOXRED1 patient cells.

Given their similarity, subsequent analysis focused on ΔFOXRED1 cells. Analysis of select steady-state levels of complex I subunits revealed that NDUFS2, NDUFS3 and NDUFV2 were strongly reduced in ΔFOXRED1 mitochondria, while the levels of subunit NDUFB6 appeared unchanged (Fig. 4E). The levels of NDUFA9, a subunit required for joining the membrane and matrix arms (33) and intermembrane space localized NDUFS5 were slightly reduced. In addition, the relative levels of select complex I assembly factors were unaltered (Fig. 4E), suggesting that the defect in complex I assembly is not due to indirect effects related to the biogenesis of these proteins. BN-PAGE analysis of mitochondria isolated from ΔFOXRED1 cells also revealed the absence of complex I in-gel activity (IGA; Fig. 4F, left panel) while respiratory complexes II, III and IV showed that the holoenzyme forms were largely unaltered. Enzyme measurements revealed that ΔFOXRED1 and ΔFOXRED1^{C2} clones displayed 13 and 11% complex I activity respectively, relative to control cells. The presence of complex III and complex IV in complex I-containing supercomplexes was severely disrupted in ΔFOXRED1 mitochondria, as expected (Fig. 4F).

ΔFOXRED1 cells exhibit a strong respiratory defect

In order to investigate the effect of the loss of FOXRED1 on respiration, we undertook analysis of OCRs and ECARs. The basal ECAR/OCR ratio was greater in ΔFOXRED1 cells, indicating an increased reliance on glycolysis for energy production in this cell

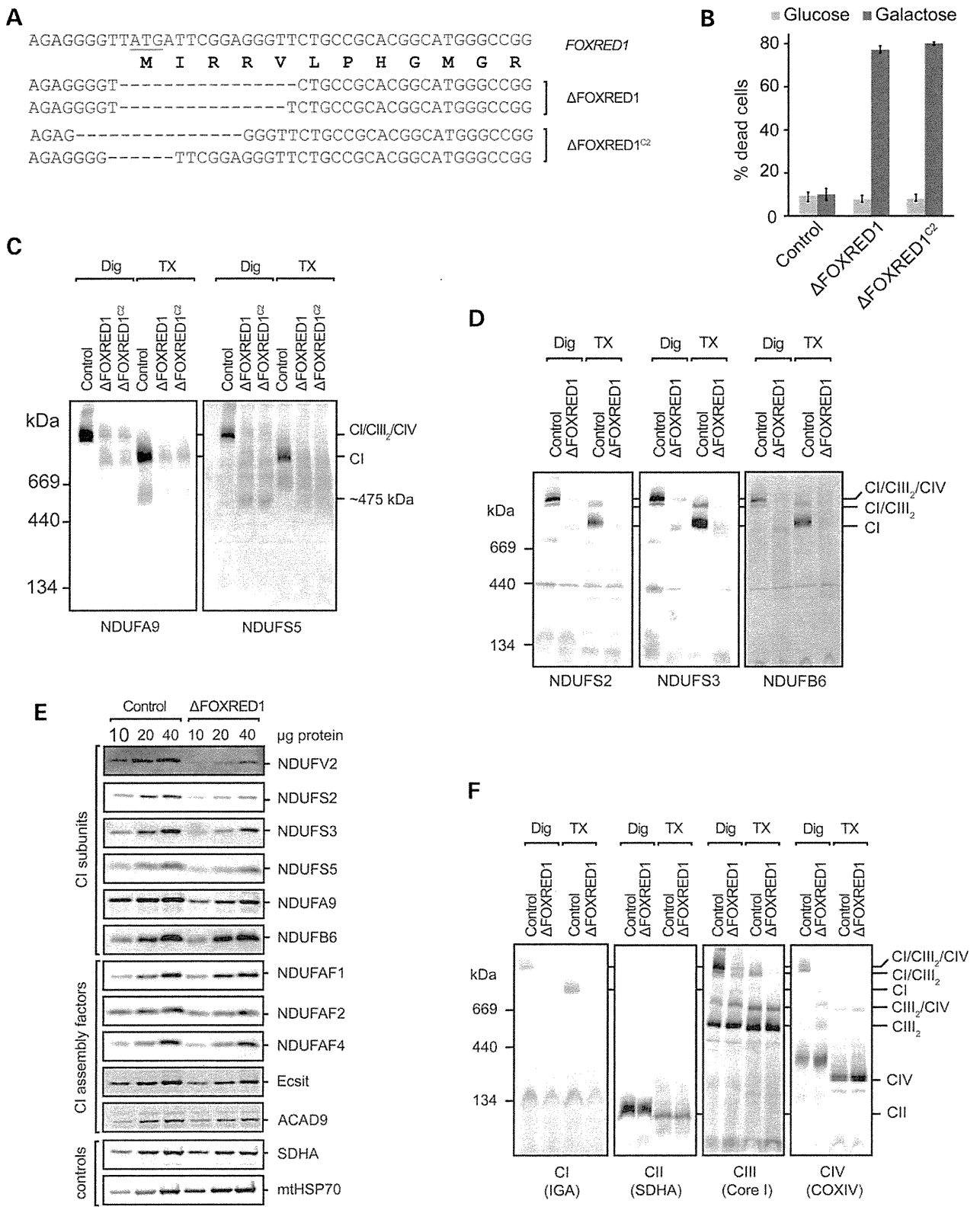

Figure 4. Generation of a ΔFOXRED1 cell line with a specific complex I defect. (**A**) Nucleotide sequence spanning the TALEN-targeted region in the *FOXRED1* gene present in the first coding exon. Sequence analyses of corresponding alleles in ΔFOXRED1 and ΔFOXRED1^{C2} cells indicate a deletion of 6–16 nucleotides encompassing the initiation codon. (**B**) Control and ΔFOXRED1 clones were plated on glucose or galactose-containing media, incubated for 72 h and analyzed for cell viability by trypan blue staining (>300 cells/assay; $n = 3$, SD). (**C**) Mitochondria isolated from control, ΔFOXRED1 and ΔFOXRED1^{C2} clones were solubilized in Digitonin (Dig) or TX before BN-PAGE followed by immunodecoration with the antibodies against complex I subunits NDUFA9 and NDUFS5. (**D**) Mitochondria isolated from control and ΔFOXRED1 cells were subjected to BN-PAGE as in (C) followed by immunodecoration with the antibodies against complex I subunits NDUFS2, NDUFS3 and NDUFB6. (**E**) Mitochondria from control and ΔFOXRED1 cells (10–40 µg protein) were subjected to SDS–PAGE and western blot analysis using antibodies against complex I subunits, assembly factors and control proteins, as indicated. (**F**) Mitochondria from control and ΔFOXRED1 cells were subjected to BN-PAGE followed by an IGA assay for complex I or western blot analysis using antibodies for complexes II (SDHA), III (Core I) and IV (COXIV).

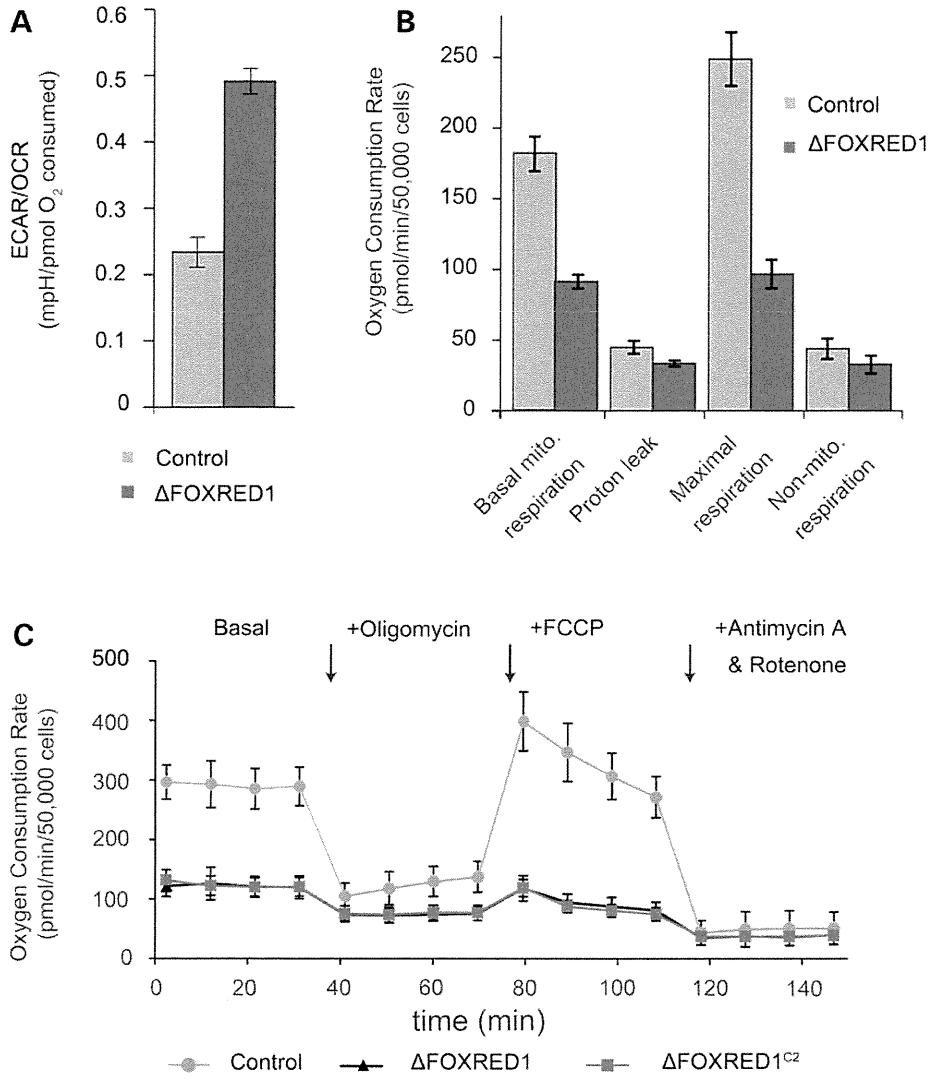

Figure 5. ΔFOXRED1 cells have a strong respiratory defect. (**A**) Measurement of the basal ECAR: basal OCR ratio for control and ΔFOXRED1 cells. ($N = 3$, SEM). (**B**) The OCR of control and ΔFOXRED1 cells was measured over a 170 min period. The addition of oligomycin was used to measure proton leak, while the maximal respiration was measured by addition of the membrane potential uncoupler FCCP. Non-mitochondrial respiration was measured by addition of rotenone and antimycin A, which inhibit CI and CIII, respectively. $N = 3$, SEM. (**C**) Representative traces of OCRs for control, ΔFOXRED1 and ΔFOXRED1^{C2} cells as described in (B). Error bars represent the SEM of 6–7 replicates/sample.

line (Fig. 5A). Further analysis of the OCR in ΔFOXRED1 cells revealed a reduced basal respiration rate, a reduced oligomycin-sensitive respiration rate due to membrane proton leak and a reduced maximal respiration rate relative to control cells (Fig. 5B). In the presence of the drugs rotenone and antimycin A, which inhibit complexes I and III, respectively, oxygen consumption was comparable, indicating no significant difference in non-mitochondrial oxygen consumption (Fig 5B). In addition, the OCRs of both ΔFOXRED1 and ΔFOXRED1^{C2} cell lines were indistinguishable (Fig. 5C). We conclude that while FOXRED1 is not essential for assembly, it is nevertheless critical for ensuring efficient complex I assembly to levels that sustain oxidative phosphorylation.

Overexpression of FOXRED1-containing pathogenic mutations can rescue assembly

Rescue studies were undertaken in order to confirm that the loss of complex I in ΔFOXRED1 cells was due to a lack of FOXRED1 protein. Transient expression of FOXRED1 fused to either a FLAG-epitope tag or GFP (both at the C-terminal end) was able to rescue the defect in complex I assembly (Fig. 6A). In addition, no defects in complex I assembly were seen following FOXRED1 overexpression in control HEK293T cells.

Two separate missense mutations have been reported in FOXRED1 that lead to complex I dysfunction—p.R352W (26) and p.N430S (25). Each mutation disrupts a highly conserved residue (Fig. 6B). Interestingly, overexpression of either FOXRED1^{R352W} or FOXRED1^{N430S} was able to rescue complex I assembly in ΔFOXRED1 cells (Fig. 6C, upper panel). Analysis by SDS–PAGE and western blotting using anti-FLAG antibodies confirmed similar expression of FOXRED1 forms (Fig 6C, lower panel). Transfected cells were also able to efficiently grow on galactose-containing media, indicating that mitochondrial respiration was restored (data not shown). These results suggest that the mutations are hypomorphic in nature.

We next undertook site-directed mutagenesis of FOXRED1 to search for key residues essential for FOXRED1 function. Mutagenesis was carried out on a subset of highly conserved tyrosine

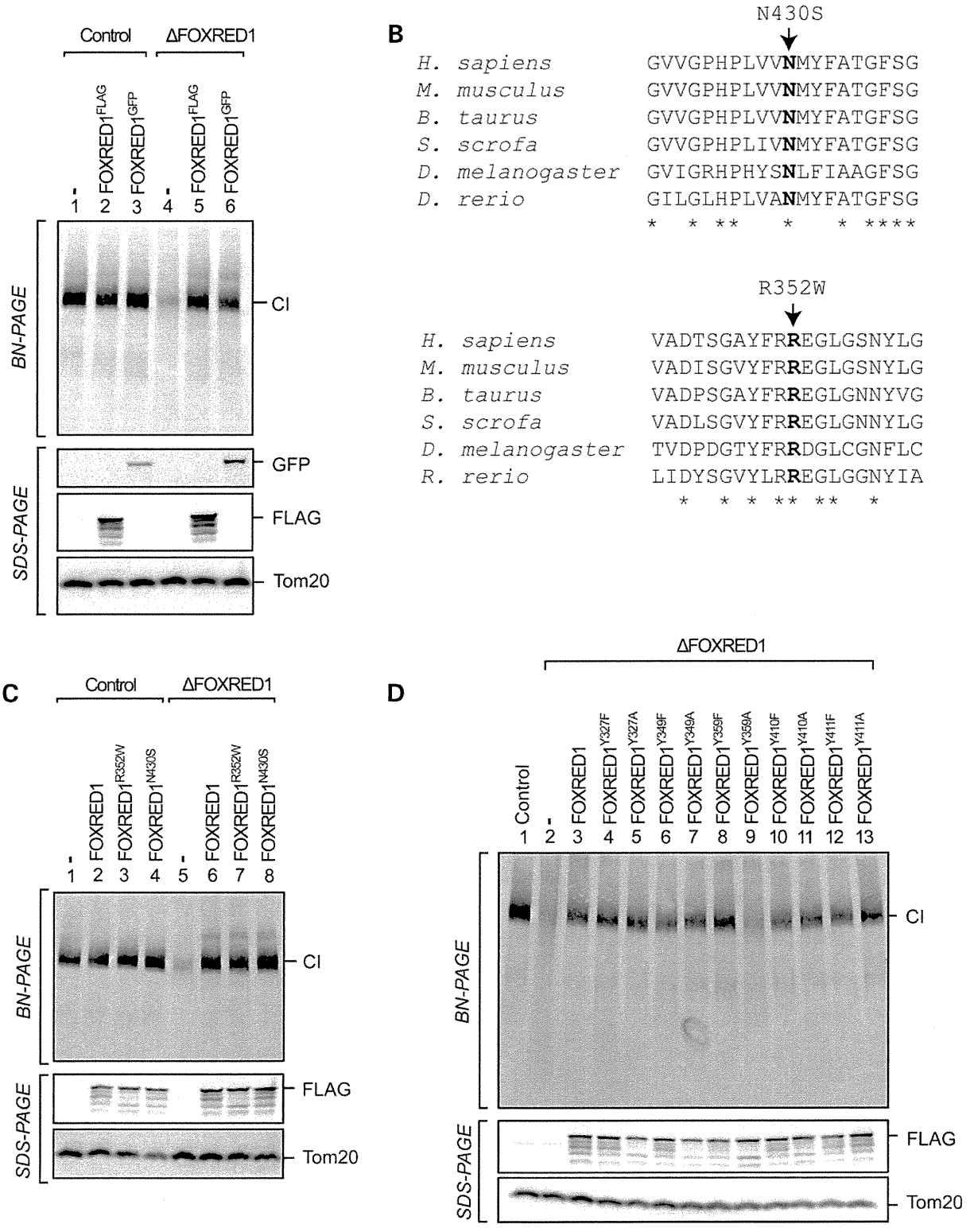

Figure 6. Complementation analysis of ΔFOXRED1 cells. (**A**) Control or ΔFOXRED1 cells expressing FOXRED1^{FLAG} or FOXRED1^{GFP} were subjected to BN-PAGE and immunoblotting with NDUFA9 antibodies to detect complex I. SDS–PAGE analysis and western blotting using FLAG and GFP antibodies was used to confirm expression of the fusion proteins. Tom20 was used as a loading control. (**B**) Partial sequence alignment of FOXRED1 from various species. The position of the patient mutations p.R352W and p.N430S is indicated. (**C**) Mitochondria isolated from control or ΔFOXRED1 cells transiently expressing FLAG-tagged FOXRED1 or patient mutations, p.R352W and p.N430S were subjected to BN-PAGE and immunoblot analysis for complex I (NDUFA9; top panel). Expression was confirmed using SDS–PAGE and immunoblot analysis with FLAG antibodies, while Tom20 was used as a loading control. (**D**) Mitochondria isolated from control or ΔFOXRED1 cells transiently expressing FLAG-tagged FOXRED1 variants were subjected to BN- and SDS–PAGE and immunoblot analysis as described in (C).